Experimental Thermal and Fluid Science 83 (2017) 19–36

Contents lists available at ScienceDirect

Experimental Thermal and Fluid Science

journal homepage: www.elsevier.com/locate/etfs

Scale effects in microscopic air-water flow properties in high-velocity free-surface flows

Stefan Felder [a,*], Hubert Chanson [b]

[a] UNSW Australia, Water Research Laboratory, School of Civil and Environmental Engineering, 110 King St, Manly Vale, NSW 2093, Australia
[b] The University of Queensland, School of Civil Engineering, Brisbane, QLD 4072, Australia

ARTICLE INFO

Article history:
Received 15 August 2016
Received in revised form 9 December 2016
Accepted 11 December 2016
Available online 16 December 2016

Keywords:
Scale effects
Air-water flow properties
Chord sizes
Cluster properties
Interparticle arrival time
Stepped spillway

ABSTRACT

Experiments of high-velocity air-water flows were conducted on two scaled stepped spillways with step heights of h = 0.05 and 0.1 m to investigate scale effects in terms of air-water flow properties for a wide range of discharges in transition and skimming flows. The investigation comprised the complete range of macroscopic and microscopic two-phase flow properties including basic air-water flow parameters, interfacial turbulence properties, as well as cluster properties based upon the near-wake criterion and interparticle arrival time. For both undistorted Froude and Reynolds similitudes, the comparative analysis highlighted scale effects in terms of several gas-liquid flow properties, demonstrating that an extrapolation to full-scale prototype conditions may not be possible. These properties comprised the interfacial area, the turbulence properties and the particle sizes and grouping, affecting any scaling of air-water mass transfer processes. Other key air-water parameters were scaled accurately including the void fraction, interfacial velocity and flow bulking. The present investigation was the most comprehensive to date providing clear guidance on air-water flow properties which may be affected by scale effects. The present results may be also applicable to other types of air-water flows. However detailed testing of air-water flow properties at the prototype scale is needed for final confirmation.

1. Introduction

With the development of faster computers the interest in numerical modelling in hydraulic engineering and fluid mechanics increased significantly. While a number of complex turbulent flow processes can be computed today, the numerical modelling of stepped spillway flows is still in its infancy despite first attempts [21,35,6,41]. Successful physical experimental studies have led to a better knowledge of stepped spillway flows and physical modelling is still the most reliable means to enhance the understanding of the micro- and macroscopic air-water flow properties and its complex interactions (Fig. 1). Stepped spillway experiments are performed with a geometric scaling ratio of the prototype stepped chute trying to reproduce the air-water flows in laboratory which would occur at full-scale (e.g. Fig. 1A). A true dynamic similarity between laboratory and prototype is not possible unless working at full scale and scale effects must be considered. In particular the scaling of air-water flows is difficult and scale effects have been reported in a variety of air-water flows in hydraulic engineering applications [34,44].

Recently Heller [33] provided a literature overview about the scaling criteria and physical modelling approaches to minimise scale effects in hydraulic engineering. While the guideline provides basic advice, the developments in terms of air-water flow scaling were restricted to void fraction and interfacial velocity. Using these two parameters Boes [5] provided earlier limited guideline of maximal scaling proportion for stepped spillway flows based upon a Froude similitude (Appendix A). Appendix A lists a number of relevant experimental studies of scale effects in stepped spillway flows. Both the instrumentation and range of investigated parameters are listed in the last two columns. In air-water flows, viscous and gravity forces are important and the assessment of scale effects cannot be limited to void fraction and interfacial velocity only. Further air-water flow properties must be considered at the time scale of air-water flow interactions, rather than the time-averaged period. The general need for large size facilities in physical modelling of air-water flows and the limitations were emphasised recently [13,37]. Indeed the results of recent experimental investigations emphasised that the selection of the criteria to assess scale affects is critical [11,16,40]. These results showed that some parameters, such as bubble sizes and turbulent scales,

* Corresponding author.
E-mail addresses: s.felder@unsw.edu.au (S. Felder), h.chanson@uq.edu.au (H. Chanson).

http://dx.doi.org/10.1016/j.expthermflusci.2016.12.009
0894-1777/

(A) Prototype scale: Paradise dam, h= 0.62 m, θ = 57.4°, d_c/h = 2.85, q = 7.4 m^2/s, Re = 2.9×10^7 (Flow from top to bottom)

(B) Laboratory scale: Present study, h= 0.05 m, θ = 26.6°, d_c/h = 2.22, q = 0.116 m^2/s, Re = 4.6×10^5 (Flow from top to bottom)

Fig. 1. Air-water flows on stepped spillways.

are likely to be affected by scale effects, even in relatively large-size laboratory models (e.g. 2:1 to 3:1). These studies comprised aerated flows in hydraulic jumps [11,16,42] and air-water flows on stepped spillways [5,17,7,25,24]. No scale effect can only be observed at full scale, when using the same fluids in prototype and model.

The present investigation extends previous findings by analysing the full range of air-water flow properties in terms of scale effects for a broad range of discharges in transition and skimming flows. The particular focus is on the microscopic air-water flow properties. The aim of this manuscript is to provide general guidance for all available air-water flow properties where scale effects may be expected in both undistorted Froude and Reynolds similitudes. Among the investigated microscopic flow properties are interparticle arrival times and cluster properties. In a detailed comparison of cluster analysis criteria, the near-wake criterion was identified as the most suitable cluster criterion and the near-wake criterion was used for the analysis of scale effects in terms of a range of cluster properties. The present results provide a clearer guidance regarding which air-water flow properties may be affected by scale effects. The outcomes may be also applicable for other types of air-water free-surface flows such as hydraulic jumps, breaking waves and drop structures.

2. Physical modelling and experimental configurations

2.1. Dimensional considerations

High-velocity air-water flows are complex two-phase turbulent flows (Fig. 1). The gas-liquid flow motion is characterised by a significant number of parameters and properties describing the dynamic processes in the high-velocity flows including the fluid properties, physical constants, two-phase flow conditions, boundary conditions and initial flow properties. A dimensional analysis of the relevant parameters can identify the most relevant dimensionless properties and parameters, including Froude, Reynolds and Weber numbers, to achieve kinematic and dynamic similarities in a geometrically-similar stepped spillway flow. Considering a steady skimming flow down a rectangular prismatic stepped chute, a simplified dimensional analysis yields a series of relationships between the air-water flow properties at a location (x, y, z) and a number of relevant dimensionless numbers:

$$\begin{aligned} & C, F \times \frac{d_c}{V_c}, \frac{V}{\sqrt{g \times d_c}}, Tu, T_{int} \times \sqrt{\frac{g}{d_c}}, \frac{L_{xz}}{d_c}, T_{xx} \times \sqrt{\frac{g}{d_c}}, a \\ & \times d_c, \frac{d_{ab}}{d_c}, \frac{ch_{cl}}{d_c}, P_{cl}, N_{cl}, F_{cl} \times \frac{d_c}{V_c}, t_{ipa} \times \sqrt{\frac{g}{d_c}}, \ldots \\ & = f\left(\frac{x}{d_c}, \frac{y}{d_c}, \frac{Z}{d_c}, \frac{d_c}{h}, Re, Mo, \theta, k_s', \ldots\right) \end{aligned} \quad (1)$$

where C is the local void fraction, F is the bubble count rate, d_c and V_c are the critical flow depth and velocity respectively: $d_c = (q_w^2/g)^{1/3}$ with q_w the specific discharge and g the gravity acceleration and $V_c = (g \times q_w)^{1/3}$, V is the interfacial velocity, Tu is an air-water flow turbulence intensity, T_{int} is an integral turbulent time scale, L_{xz} is a turbulent length scale, T_{xx} is an auto-correlation time scale, a is the specific interface area, d_{ab} is a chord size of entrained particles, ch_{cl} is the average chord size of particles in clusters, P_{cl} is the percentage of particles in clusters, F_{cl} is the number of clusters per second, t_{ipa} is the interparticle arrival time, x, y and z are the longitudinal, normal and transverse directions respectively, h is the step height, Re is the Reynolds number defined in terms of the hydraulic diameter, Mo is the Morton number, θ is the chute slope and k_s' is the step surface roughness height. More details about the definition of the air-water flow properties in Eq. (1) can be found in Felder [24] and Felder and Chanson [27]. In Eq. (1), d_c/h is the dimensionless discharge proportional to a Froude number defined in terms of the step height since: $d_c/h = (q_w^2/(g \times h^3))^{1/3}$, and Mo is the Morton number: $Mo = g \times \mu^4/(\rho \times \sigma^3)$, with ρ and μ the water density and dynamic viscosity, and σ the surface

tension between air and water. The Morton number links the Weber and Reynolds numbers in air-water flows if the same liquids are used in the scaled models [34,44,37], and only Froude and Reynolds numbers become independent.

In practice it is not possible to satisfy simultaneously Froude and Reynolds similitude in a scaled model when the same fluids (air and water) are used in model and prototype [38,44] and a true similarity cannot be achieved. Satisfying either Froude or Reynolds similitude, a detailed testing of potential scale effects is required to provide guidance on scalability of flow properties. For a two-dimensional air-water flow down a given stepped chute, the chute slope, the macro-roughness of the invert and Morton number are invariant. Thus Eq. (1) becomes:

$$C, F \times \frac{d_c}{V_c}, \frac{V}{\sqrt{g \times d_c}}, Tu, T_{int} \times \sqrt{\frac{g}{d_c}}, \frac{L_{xz}}{d_c}, T_{xx} \times \sqrt{\frac{g}{d_c}}, a \times d_c, \frac{d_{ab}}{d_c}, \frac{ch_{cl}}{d_c}, P_{cl}, N_{cl}, F_{cl} \times \frac{d_c}{V_c}, t_{ipa} \times \sqrt{\frac{g}{d_c}}, \ldots = f\left(\frac{x}{d_c}, \frac{y}{d_c}, \frac{d_c}{h}, Re\right), \quad (2)$$

In the present study, a systematic investigation of a wide range of air-water flow properties (Eq. (2)) was conducted to test scaling criteria for both undistorted Froude and Reynolds similitudes on stepped spillways. In a laboratory stepped spillway facility, two geometrically scaled models were tested with a scaling ratio of 1:2 comprising step heights of h = 0.05 m (20 steps) and h = 0.1 m (10 steps) (Appendix A). Both stepped configurations were installed in the same test section with channel slope of $\theta = 26.6°$, channel width of 1 m and identical smooth inflow conditions via a broad-crested weir at the upstream end.

2.2. Experimental data sets

The experimental data set was obtained for a range of discharges in transition and skimming flow regimes ($0.69 \leqslant d_c/h \leqslant 3.3$; $8.1 \times 10^4 \leqslant Re \leqslant 9 \times 10^5$) to enable the extrapolation of results for several flow conditions and to allow the application of the scaling guidelines of the present study to further air-water free-surface flows. For both flow regimes, the water was non-aerated at the upstream end and became aerated downstream of the inception point of free-surface aeration where the turbulence fluctuations close to the surface overcame buoyancy and surface tension forces (Fig. 1B). Downstream of the inception point the flow consisted of a complex mixture of air and water entities which were continuously entrained and detrained through the free-surface. For design flow conditions corresponding to a skimming flow regime, the water skimmed over the step edges with a free-surface parallel to the pseudo-bottom formed by the step edges (Fig. 1B). Within the step cavities, strong three-dimensional recirculation took place which dissipated some of the flow energy. For the transition flow regime, the flows were less stable with some irregular motions and ejections in the step cavities and strong splashing of droplets [19,24]. Visual observations of the flow patterns for the two scaled models did not show any discernible differences in air-water flow motions for the respective flow regime.

For both transition and skimming flow regimes, detailed experiments were conducted downstream of the inception point of free-surface aeration using phase-detection intrusive probes. Two types of probes were used comprising double-tip conductivity probes with a longitudinal sensor distance of $\Delta x = 7.2$ mm and two identical single-tip conductivity probes which were separated by a range of transverse distances ($3.3 \leqslant \Delta z \leqslant 80.8$ mm). The single-tip probes had diameters of the inner electrode of 0.35 mm and the double-tip probe sensors had diameters of 0.25 mm. All sensor pairs were sampled simultaneously at 20 kHz per sensor for 45 s [27]. The piercing of air or water entities by the probe sensors resulted in specific Voltage signals reflecting the different resistivity of air or water. The raw Voltage signals were post-processed using a single-threshold technique and correlation analyses providing the full range of air-water flow properties. Further details about the signal processing can be found in Felder [24]. The resulting air–water flow properties are defined in more detail in Sections 3 and 4, including the various cluster properties calculated with three different cluster analysis criteria.

3. Air-water flow properties

3.1. Basic observations

Basic air-water flow properties were recorded with the double-tip conductivity probe for all flow conditions in transition and skimming flows. Distributions of these properties are illustrated in Fig. 2 highlighting typical observations of air-water flow characteristics. All data are illustrated in dimensionless form as function of the dimensionless flow depth y/Y_{90} where Y_{90} is the flow depth where C = 0.9. Fig. 2A illustrates typical void fraction distributions for several consecutive step edges highlighting typical S-shape distributions with small void fractions close to the step edge in the bubbly flow region ($C < 0.3$), a rapid increase of void fractions in the intermediate flow region ($0.3 < C < 0.7$) and void fractions approaching unity in the spray region close to the free-surface ($C > 0.7$). The observations were consistent with previous studies on stepped spillways including a close agreement with the advective diffusion equation for air bubbles [19]. Distributions of dimensionless bubble count rate $F \times d_c/V_c$ are shown in Fig. 2B for several consecutive step edges. Close to the step edge, the number of air bubbles was small (Fig. 2B). The bubble count rate increased with increasing void fraction and vertical distance from the step edge up to a maximum number of air bubbles in the intermediate flow region. In the upper spray region, the bubble count rate decreased to very small values linked with only small numbers of ejected water droplets impacting the probe tips. With increasing distance downstream of the inception point of free-surface aeration, the number of entrained air bubbles increased (Fig. 2B).

The dimensionless distributions of time-averaged interfacial velocity V/V_{90}, where V_{90} is the velocity where C = 0.9, showed also typical features which agreed reasonable well with a power law with an exponent of 1/10th on average (Fig. 2C). Some small variations in the exponent were observed between adjacent step edges. Fig. 2C illustrates the V/V_{90} distributions for all flow rates on the stepped spillway with h = 0.05 m as a function of y/Y_{90}. For $y/Y_{90} > 1$, the velocity profiles were uniform as previously reported [2,26].

Typical distributions of turbulence levels Tu are illustrated in Fig. 2D for several consecutive step edges downstream of the inception point of air entrainment. The distributions agreed with previous observations of largest turbulence intensities in the intermediate flow region and turbulent levels close to mono-phase flow values in lower bubbly and upper spray regions [36,1]. The strong air-water turbulence interactions in the flow region with same entities of air and water confirmed the importance of the intermediate flow region in terms of turbulent energy dissipation processes which were believed to be closely linked with the interfacial aeration. The turbulence levels within the bulk of the air-water flows were between 100 and 140% (Fig. 2D).

Further details regarding the basic air-water flow properties and some advanced air-water flow properties for both transition and skimming flows were recently presented by Felder and Chanson [27] for the same stepped spillway facility. In addition to the

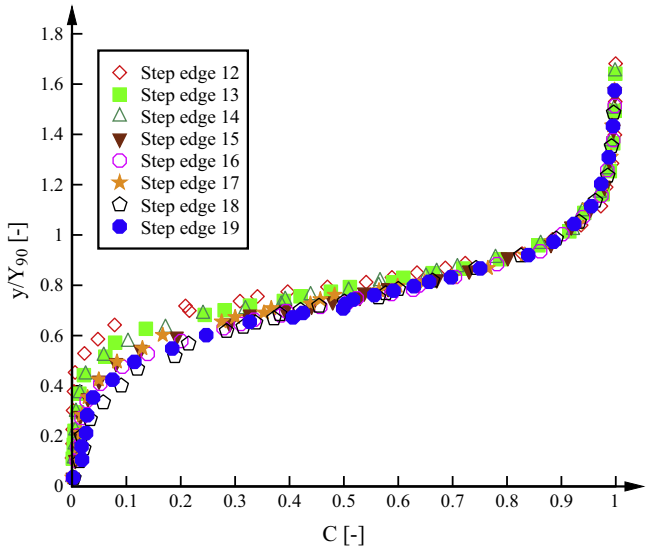

(A) Void fraction: $d_c/h = 2.22$; $q_w = 0.116$ m^2/s; Re $= 4.6\times10^5$; h = 0.05 m

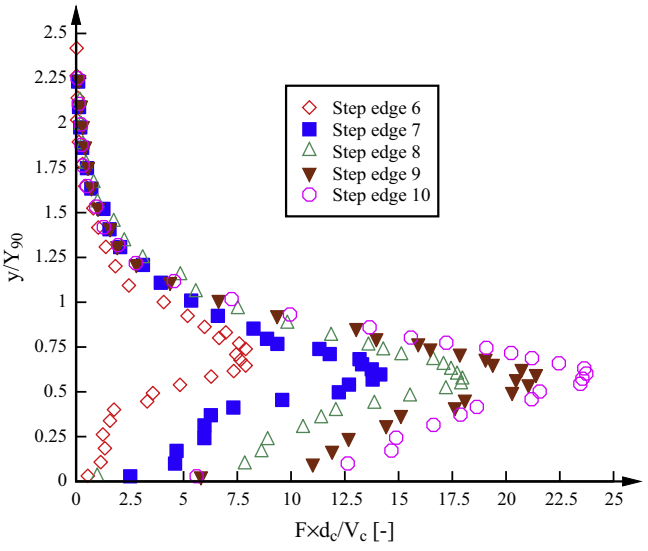

(B) Bubble count rate: $d_c/h = 1.11$; $q_w = 0.116$ m^2/s; Re $= 4.6\times10^5$; h = 0.1 m

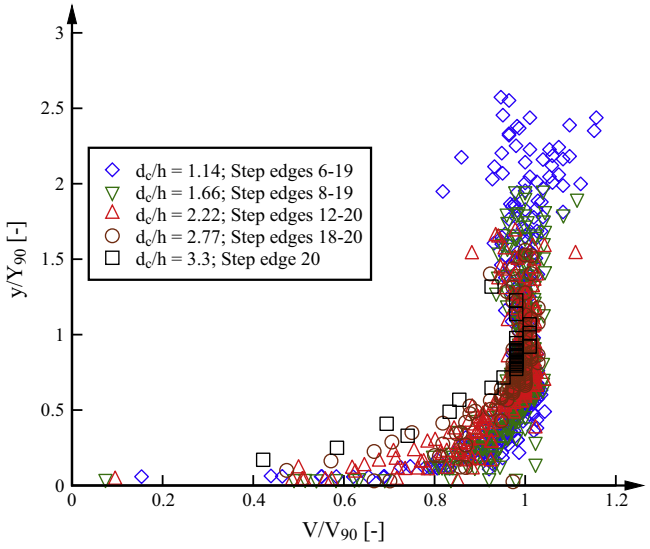

(C) Interfacial velocity: $0.7 \le d_c/h \le 3.3$; $0.02 \le q_w \le 0.21$ m^2/s; $8.1\times10^4 \le$ Re $\le 4.6\times10^5$; h = 0.05 m

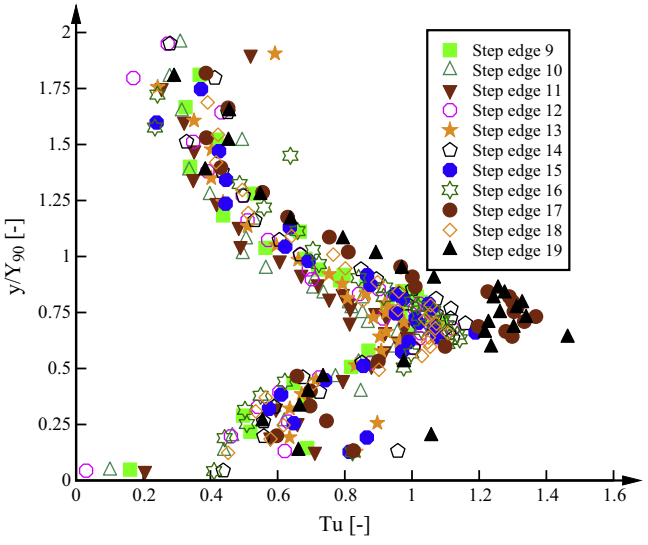

(D) Turbulence intensity: $d_c/h = 1.66$; $q_w = 0.075$ m^2/s; Re $= 3\times10^5$; h = 0.05 m

Fig. 2. Distributions of basic air-water flow properties on a stepped spillway in skimming flows.

basic air-water flow properties presented in this section, the results of Felder and Chanson [27] included observations of maximum cross-correlation coefficient in a cross-section $(R_{xy})_{max}$, auto- and cross-correlation integral time scales, air bubble and water droplet chord sizes, transverse integral turbulent time and length scales and advection length scale. All these basic and advanced air-water flow properties were used for the comparative analyses of scale effects (Section 4). In addition further microscopic air-water flow properties comprised bubble and droplet clustering. In the following section (Sections 3.2 and 3.3), the most appropriate cluster definition criterion is identified.

3.2. Cluster analyses

Cluster analysis based upon a single sensor tip can provide information about the microscopic structure of the air-water flows in streamwise direction [32]. Herein a comparative analysis was undertaken of three typical cluster analysis criteria comprising a range of air-water cluster properties. Air bubbles and water droplets were considered as travelling in a cluster if the air/water chord length between two adjacent particles was smaller than a characteristic length scale. In previous air-water flow studies on stepped spillways, plunging jets and hydraulic jumps, three different cluster criteria were used to define the characteristic scale between adjacent particles (Table 1). The cluster criteria comprised a constant length scale of 1 mm, a length scale of 10% of the mean chord size and the near-wake criterion (Table 1).

In the near-wake criterion, a cluster occurred when the length scale between successive air bubbles or water droplets L_{cl} was smaller than the size of the leading bubble/droplet ch_{lead}:

$$\omega \times ch_{lead} > L_{cl} \quad (3)$$

Table 1
Summary of experimental studies of one-dimensional cluster properties in air-water flows.

Reference	Flow type	Cluster criterion	Cluster properties
Chanson and Toombes [18]	Stepped spillway	Constant length scale: 1 mm	N_{cl}; P_{cl}; ch_{cl}/ch
Chanson and Toombes [19]	Stepped spillway	10% of mean chord size	N_{cl}; P_{cl}; ch_{cl}/ch
Gualtieri and Chanson [30]	Drop shaft	10% of mean chord size	N_{cl}; P_{cl}; F_{cl}
Chanson et al. [14]	Plunging jet	Near-wake	N_{cl}; P_{cl}; F_{cl}
Chanson [12]	Hydraulic jump	10% of mean chord size	N_{cl}; P_{cl}; F_{cl}; PDF of N_{cl}
Gualtieri and Chanson [31]	Hydraulic jump	10% of mean chord size Near-wake	N_{cl}; P_{cl}; F_{cl}
Wang and Chanson [42]	Hydraulic jump	Near-wake	N_{cl}; P_{cl}; F_{cl}; PDF of N_{cl}
Present study	Stepped spillway	Constant length scale: 1 mm 10% of mean chord size Near-wake	N_{cl}; P_{cl}; F_{cl}; PDF of N_{cl}; ch_{cl}; ch_{cl}/ch

where the factor ω represents the wake time scale ratio often selected within the range $\omega = 0.5–2$ for pseudo-spherical particles [22]. Herein $\omega = 1$ was selected following Chanson et al. [14]. The near-wake criterion relied on the local characteristic flow scales [31].

A further cluster criterion identified the particles as travelling in clusters by defining the characteristic scale between two adjacent particles in a cluster as 10% of the mean chord size ch_{mean} [19]:

$$\frac{1}{10} \times ch_{mean} > L_{cl} \quad (4)$$

Chanson and Toombes [18] used a further cluster criterion based upon a constant length scale of 1 mm below which particles were considered as travelling in clusters. It was argued that this length scale was about 20–50 times smaller than the mean water chord length in the bubbly flow region [18] and for consistency a constant length scale of 1 mm was used in the present study. As shown by Felder and Chanson [28], a wide range of time scales are characteristic for air-water flows on stepped spillways making it difficult to select a constant time scale for all flow regions limiting the application of a constant criterion. These limitations are further discussed in Section 3.3.

For all three cluster criteria, cluster properties were calculated in two flow regions comprising bubbly flows ($C < 0.3$) and spray region ($C > 0.7$) [9,28]. A range of cluster properties were calculated comprising the percentage of bubbles/droplets in clusters P_{cl}, the number of clusters per second F_{cl}, the average number of particles per cluster N_{cl}, the average chord size of particles in clusters ch_{cl}, the ratio of average chord size of particles in clusters ch_{cl} and average chord size ch, as well as the probability distribution function (PDF) of the number of particles per cluster. Table 1 summarises the cluster properties investigated in previous and present studies.

The cluster properties for the three cluster criteria are presented in Fig. 3, showing typical results observed for transition and skimming flow conditions. For all cluster properties, significant differences between the cluster criteria were found (Fig. 3). In Fig. 3A, the percentage of particles in clusters P_{cl} is illustrated as a function of the void fraction. For the near-wake criterion, the percentage of particles in clusters was very small for $C \approx 0$ and $C \approx 1$ and increased linearly with change in void fractions. For $C = 30\%$ and $C = 70\%$, the maximum percentage of particles in clusters was about 60%. The criterion with 10% of mean chord size showed opposite trends with largest percentage of particles in clusters for $C \approx 0$ and $C \approx 1$. In the bubbly flow region ($C \approx 0$), a maximum of 25–30% of bubbles were in clusters and in the upper spray region ($C \approx 1$), the maximum percentage of droplets in clusters was about 50–70%. The percentage of particles in both bubbly and spray regions decreased linearly to about 10% for $C \approx 0.3$ and $C \approx 0.7$. For the constant criterion, the percentage of particles in clusters was almost uniform with about 10–20% of particles in clusters.

For the number of clusters per second F_{cl}, large differences between the cluster criteria were also observed (Fig. 3B). While the distributions had similar shapes with very small number of clusters per second for $C \approx 0$ and $C \approx 1$, the increase in clusters per second towards the intermediate flow region differed significantly. For the near-wake criterion much larger numbers of clusters per second were observed for $C = 0.3$ and $C = 0.7$ with maxima about 5 times larger compared to the percentage criterion and about 8 times larger compared to the constant criterion. Similarly major differences were observed in terms of the number of particles per cluster N_{cl} (Fig. 3B). For the near-wake criterion, the number of particles per cluster increased from 2 particles close to the step edge and at the free-surface to average numbers of particles of about 2.5–3 in the intermediate flow region. In contrast for the criterion with 10% of the mean chord size, the number of particles per cluster increased from 2 particles per cluster in the intermediate flow region to about 2.5 particles for $C \approx 0$ and $C \approx 1$ respectively. For the constant cluster criterion, the average number of particles was smaller for all void fractions and was almost constantly 2 particles (Fig. 3B). Detailed probability distribution functions of the number of particles per cluster are illustrated in Fig. 3C for bubbles and Fig. 3D for droplets. For the constant and percentage criteria, the probability distributions of particles were close with 80–95% of clusters having 2 particles. Only a small percentage of clusters had 3 or more particles (Fig. 3C & D). In contrast, the near-wake criterion exhibited overall clusters with larger numbers of particles per cluster. Clusters could comprise up to 9 particles, while about 60–70% of clusters consisted of 2 particles only.

Characteristic distributions of the average chord sizes of particles in clusters and of the ratio of average chord sizes of particles in clusters to average chord sizes are compared in Fig. 3E and F respectively for the three cluster criteria. For all chord size distributions, the distributions for the criteria with constant scale and with scale of 10% of the mean chord were in close agreement with increasing chord sizes towards the intermediate flow region (Fig. 3E) and almost constant ratio of chord sizes across the air-water flow column (Fig. 3F). For the near-wake criterion, the shapes of the chord size distributions were similar. However the average chord sizes of particles in clusters were consistently larger by about 15–30% and the ratio of chord sizes of clusters to chord sizes was about 20% larger (Fig. 3F).

3.3. Discussion

All cluster criteria identified a significant number of bubbles and droplets travelling in clusters in the bubbly and spray flow regions. The comparison of the cluster properties showed significant differences between the three cluster criteria linked with the definition of the characteristic scale between adjacent particles. For the criterion with the scale of 10% of the mean chord size, the criterion was affected by the different number of air-water

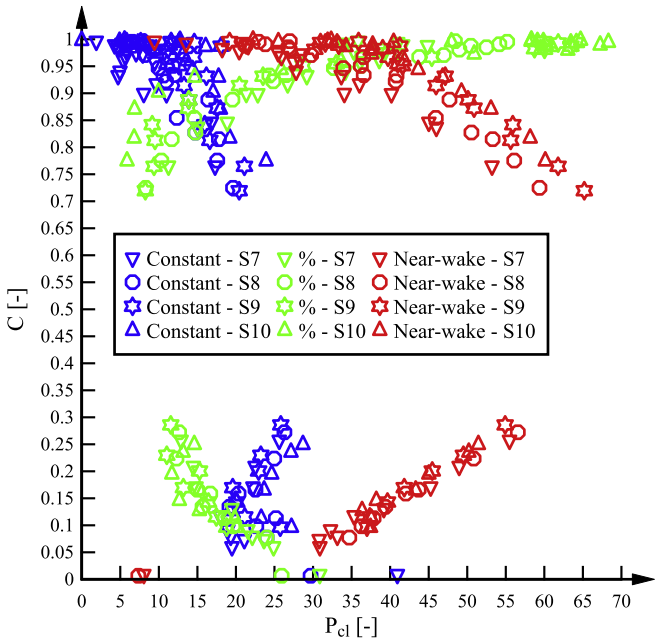

(A) Percentage of particles in clusters P_{cl}: d_c/h = 0.83; h = 0.1 m

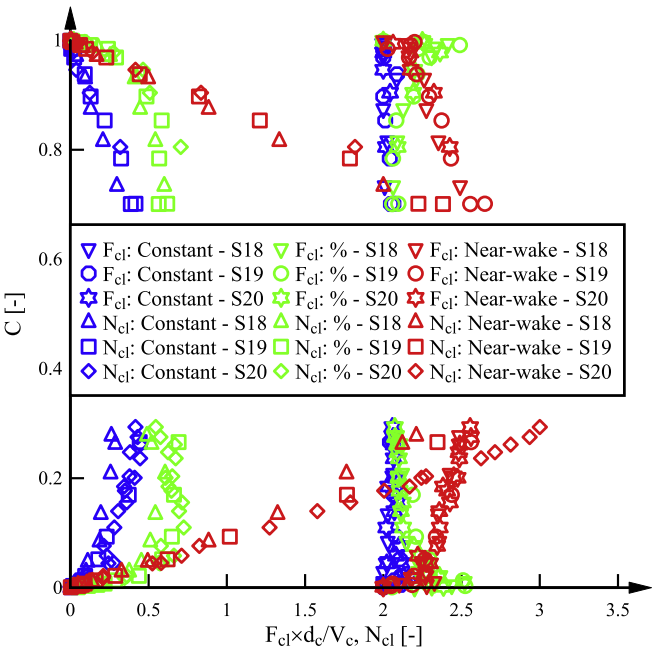

(B) Number of particles per cluster N_{cl} and cluster per second F_{cl}: d_c/h = 2.77, h = 0.05 m

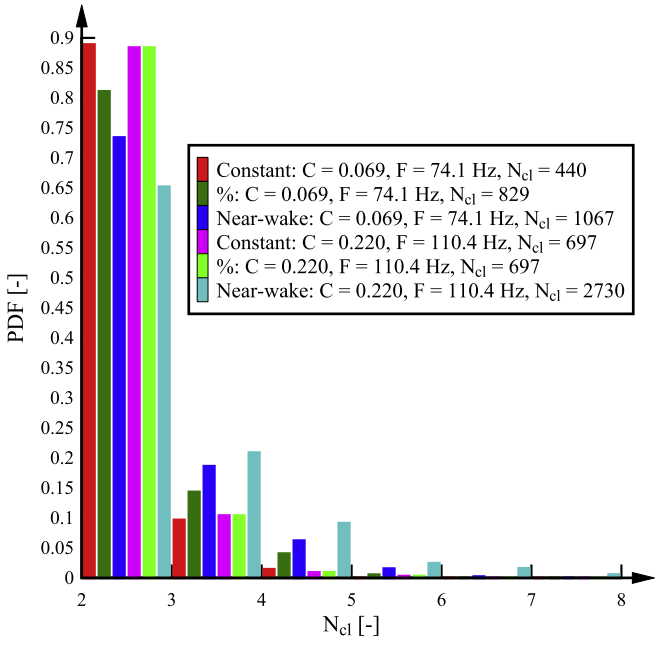

(C) PDF of bubbles per clusters N_{cl}: d_c/h = 1.49; h = 0.1 m

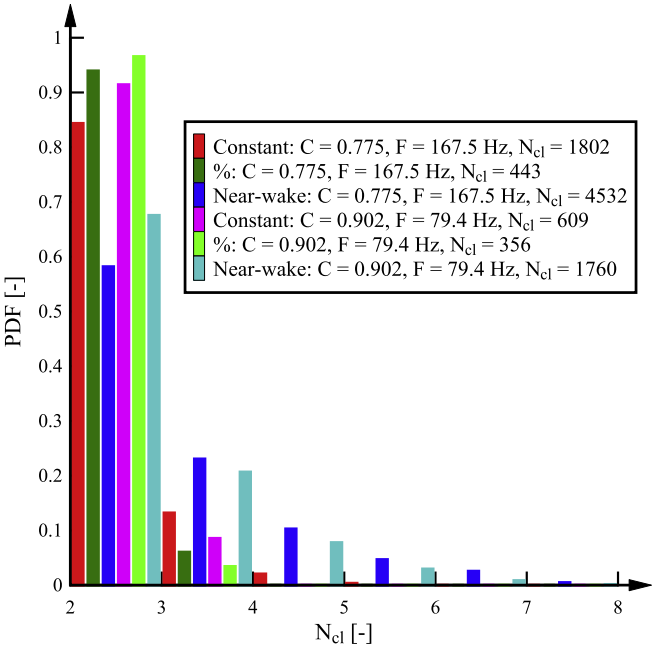

(D) PDF of droplets per clusters N_{cl}: d_c/h = 0.83; h = 0.1 m

Fig. 3. Comparison of cluster properties for three cluster criteria.

interfaces. For example, for a position close to the step edge with small void fraction and small number of bubbles, the mean water chord size between two adjacent bubbles was much larger compared to a region with larger void fraction and larger bubble count rate close to the intermediate flow region (C = 0.3). A larger characteristic cluster scale between adjacent air bubbles led to a larger percentage of bubbles in clusters and to a larger number of bubbles per cluster. The application of this criterion is therefore strongly affected by the number of air-water interfaces and the positioning within the air-water flows.

For the constant criterion, a sensitivity analysis was conducted for time scales between 1 and 10 ms reflecting the variety of characteristic time scales in air-water flows on stepped spillways. While the sensitivity analysis is not presented in this manuscript, the results suggested that the percentage of particles in clusters, the average number of particles per cluster and the number of clusters per second were sensitive to the selection of the constant scale. In contrast the chord size properties of particles in clusters were less sensitive and had little effect on the distributions. More details can be found in Felder [24]. Overall the sensitivity analysis

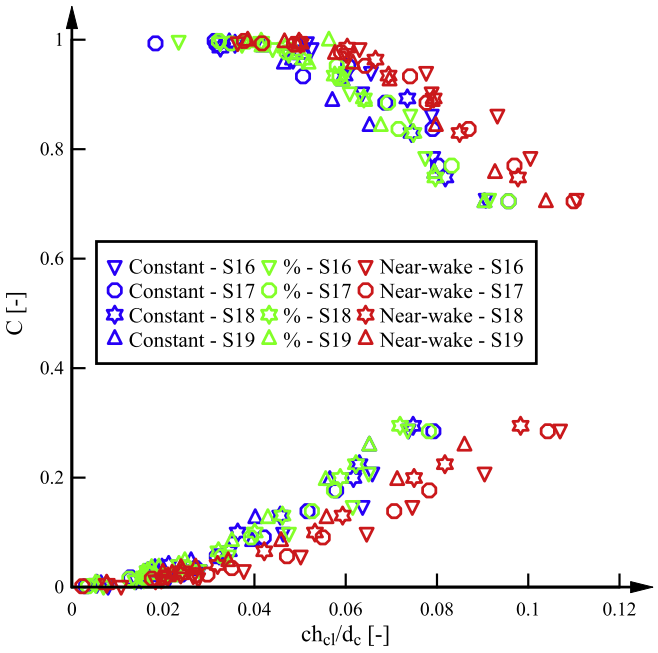

(E) Average chord size of particles in clusters ch_{cl}: $d_c/h = 2.22$, $h = 0.05$ m

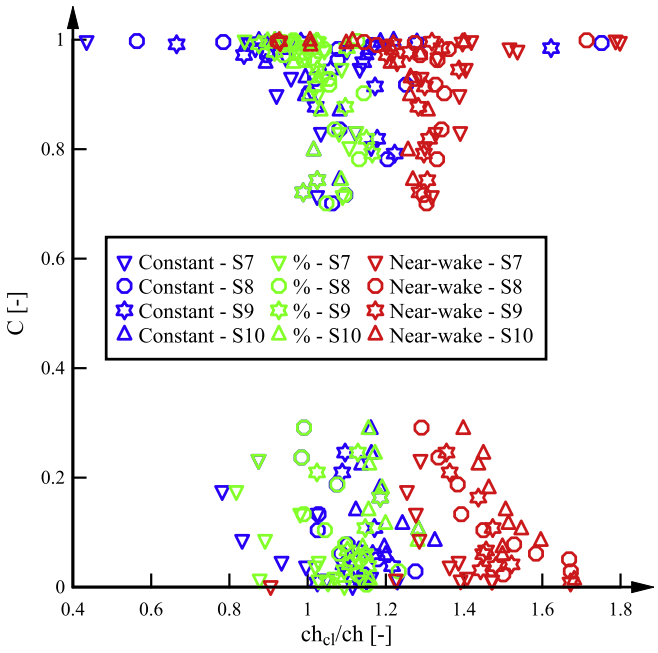

(F) Ratio of average chord size of cluster particles ch_{cl} to average chord size ch: $d_c/h = 1.28$; $h = 0.1$ m

Fig. 3 (*continued*)

confirmed that cluster properties are affected by the choice of the constant length/time scale and that such a criterion may be unsuitable for air-water flows on stepped spillways. This aspect is strengthened by Felder and Chanson [28] who highlighted the range of characteristic time scales affecting the air-water flows in various regions of the flow.

The characteristic scale for the near-wake criterion was identified based upon the lead particle size in a cluster. Therefore, this criterion was linked with the local flow characteristics and the number of air-water interfaces at each location within a cross-section. The close relationship between number of clusters per second and the bubble count rate confirmed the physical meaning of the near-wake criterion. For all data, independently of the flow rate, of the distance downstream of the inception point and of the step height, a close relationship was observed between dimensionless bubble count rate and dimensionless number of bubble clusters per second (Fig. 4A) and number of droplet clusters per second respectively (Fig. 4B). The best fit correlation between bubble count rate and number of bubble clusters per second was (R = 1):

$$F \times d_c/V_c = 0.4754 + 4.542 \times F_{cl} \times d_c/V_c \quad \text{bubbly flow} \tag{5}$$

and the relationship for the water droplets was best expressed by (R = 0.96):

$$F \times d_c/V_c = 1.647 + 4.826 \times F_{cl} \times d_c/V_c \quad \text{spray region} \tag{6}$$

For comparison, in Fig. 4 the corresponding data for the cluster criteria with constant length scale and 10% of the mean chord size are added. For both criteria, a large data scatter was found as well as differences between different step heights.

Overall the near-wake criterion appeared to be best suited to characterise the cluster flow properties in the bubbly and spray flow regions. The finding is in agreement with the observations of Gualtieri and Chanson [31] in a hydraulic jump. The near-wake criterion was therefore used in the investigation of scale effects of cluster properties.

4. Scale effects in high-velocity free-surface flows

A systematic investigation of scale effects was conducted for both Froude and Reynolds similitudes. The experimental flow conditions are summarised in Tables 2 and 3 comprising information about the dimensionless discharge d_c/h, the discharge per unit width q_w, the corresponding Reynolds number as well as information about the measured step edges and the inception point of free-surface aeration for both transition (TRA) and skimming (SK) flow regimes. The comparison of scale effects was always conducted at the same relative distance downstream of the inception point of air entrainment. The comparative analysis comprised a wide range of air-water flow properties for both Froude and Reynolds similitudes over a range of flow conditions (Tables 2 and 3).

4.1. Froude similitude

A comparison of a range of air-water flow properties is illustrated in Fig. 5 for the geometrically scaled stepped spillways for both transition and skimming flows. All data are shown in dimensionless terms for several consecutive step edges as a function of the dimensionless distance perpendicular to the main flow direction y/d_c. While most properties showed some disagreement between the scaled spillway models, the important parameter of void fraction showed good agreement (Fig. 5A) and no scale effects were observed for the Froude similitude for the investigated range of Reynolds numbers (Table 2). The findings were consistent with observations of void fractions on geometrically scaled stepped spillways with slopes of $\theta = 3.4°$ and $\theta = 15.9°$ [17], with $\theta = 21.8°$ [25] and with slopes of $\theta = 30°$ and $50°$ [5].

Very close agreement was also observed for the maximum cross-correlation coefficient in a cross-section $(R_{xy})_{max}$ which was scalable based upon a Froude similitude (Fig. 5B). In contrast, the comparison of auto- and cross-correlation functions showed slightly larger correlation functions for the 0.1 m high steps in the bubbly flow region ($C < 0.3$) and in the spray region the

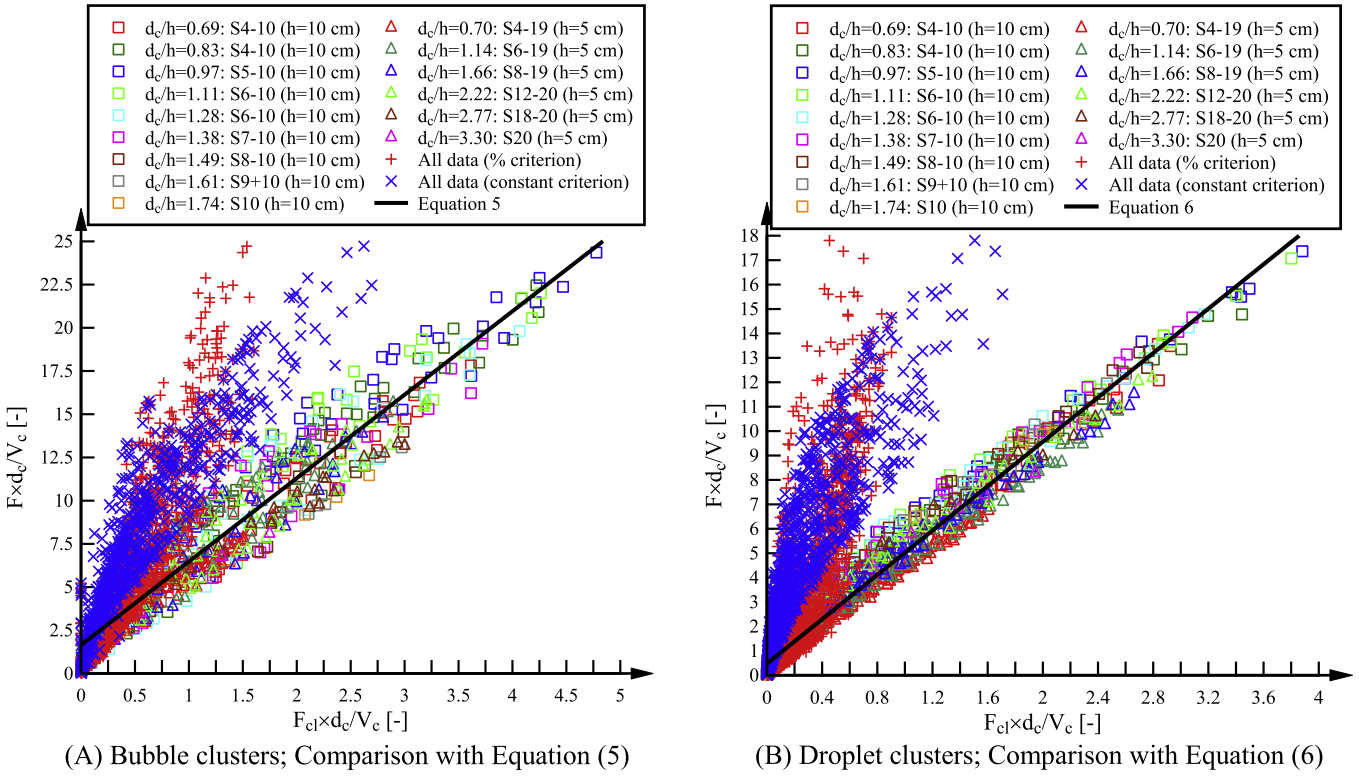

Fig. 4. Comparison of relationship between number of clusters per second and bubble count rate for the three cluster analysis criteria.

Table 2
Experimental flow conditions for comparison of air-water flow properties based upon Froude similitude.

Step height: h = 0.1 m					Step height: h = 0.05 m				
d_c/h [–]	q_w [m^2/s]	*Re* [–]	Flow regime	Incep. point	d_c/h [–]	q_w [m^2/s]	*Re* [–]	Flow regime	Incep. point
0.69	0.056	2.2×10^5	TRA	3–4	0.7	0.020	8.1×10^4	TRA	4
1.11	0.116	4.6×10^5	SK	6	1.14	0.042	1.7×10^5	SK	6–7
1.61	0.202	8.0×10^5	SK	9–10	1.66	0.075	3.0×10^5	SK	8–9

Table 3
Experimental flow conditions for comparison of air-water flow properties based upon Reynolds similitude.

Step height: h = 0.1 m					Step height: h = 0.05 m				
d_c/h [–]	q_w [m^2/s]	*Re* [–]	Flow regime	Incep. point	d_c/h [–]	q_w [m^2/s]	Re [–]	Flow regime	Incep. point
0.83	0.075	3.0×10^5	TRA	4	1.66	0.075	3.0×10^5	SK	8 to 9
1.11	0.116	4.6×10^5	SK	6	2.22	0.116	4.6×10^5	SK	12
1.38	0.161	6.4×10^5	SK	7 to 8	2.77	0.161	6.4×10^5	SK	18
1.61	0.202	8.0×10^5	SK	9 to 10	3.3	0.210	8.3×10^5	SK	20

correlation functions were slightly larger for the smaller steps. These observations are not illustrated in this manuscript but can be found in Felder [24]. A very close agreement between the two scaled models was also observed in terms of the dimensionless interfacial velocity V/V_c (Fig. 5B) which showed that the velocities were properly scaled with a Froude similitude for both transition and skimming flow regimes. The results confirmed observations by Boes [5], Chanson and Gonzalez [17] and Felder and Chanson [25] in their studies of skimming flows on stepped spillways.

All other air-water flow properties in Fig. 5 showed some sale effects for both flow regimes. Significant differences were observed for the bubble count rate distributions $F \times d_c/V_c$ (Fig. 5C). For the smallest step heights, the dimensionless bubble count rates were typically half the size of the complementing bubble frequencies for the larger step heights. The Froude similitude did not scale the number of entrained air bubbles accurately. This finding was consistent with the observations by Chanson and Gonzalez [17] and Felder and Chanson [25] in their stepped spillway experiments. A closely related property is the specific interfacial area $a \times d_c$ which also showed significant scale effects for the investigated flow conditions (Fig. 5C). Both bubble count rate and interfacial area are closely linked with air-water mass transfer processes highlighting that the air-water mass transfer cannot be properly scaled with a Froude similitude.

A range of turbulence properties were calculated following definitions by Chanson and Toombes [19] and Chanson and Carosi [15]. For both transition and skimming flow discharges, all turbulence properties showed scale effects comprising the turbulence intensity Tu (Fig. 5A), the auto- and cross-correlation time scales $T_{xx} \times (g/d_c)^{1/2}$ and $T_{xy} \times (g/d_c)^{1/2}$ (Fig. 5D), the transverse integral

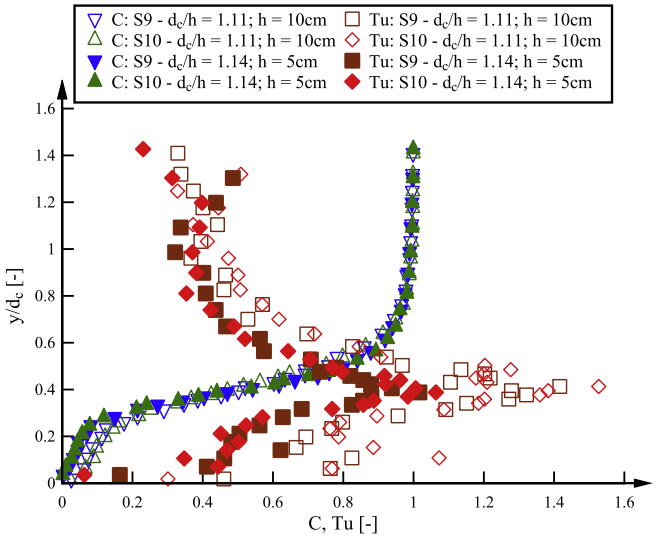

(A) Void fraction and turbulence intensity

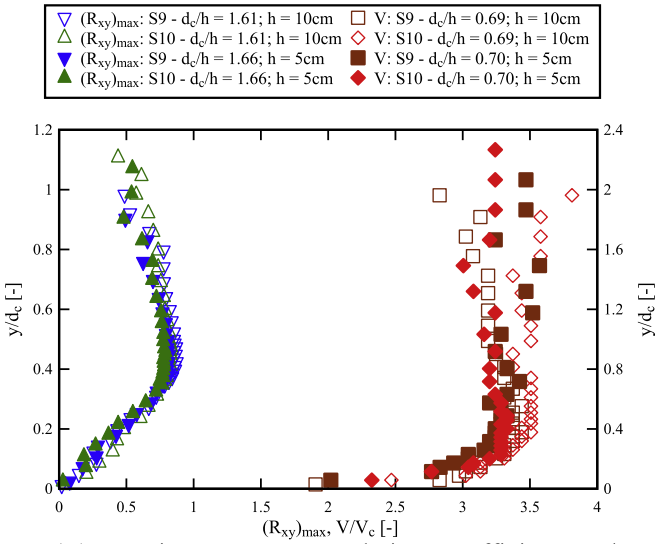

(B) Maximum cross_correlation coefficient and interfacial velocity

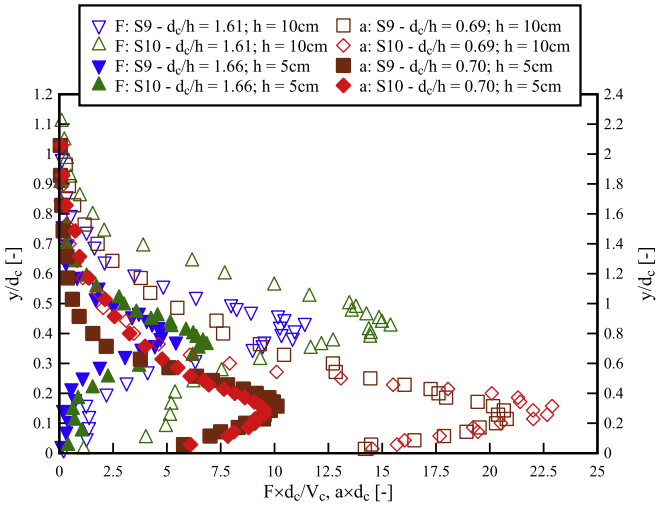

(C) Bubble count rate and interfacial area

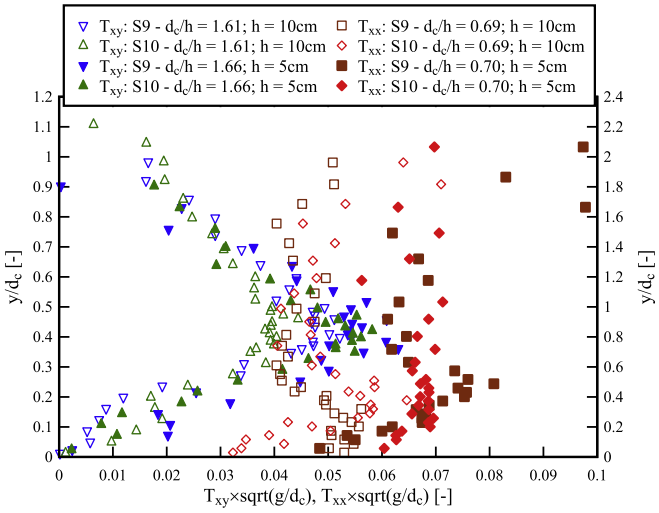

(D) Auto- and cross-correlation time scales

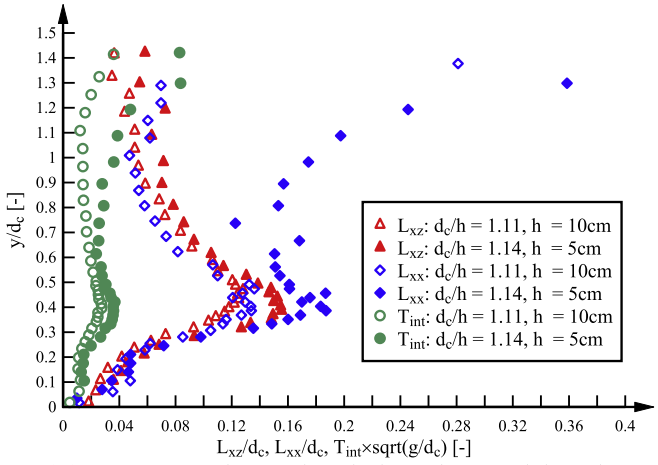

(E) Transverse integral turbulent time and length scales; advection length scale

Fig. 5. Comparison of air-water flow properties based upon Froude similitude.

turbulent time and length scales $T_{int} \times (g/d_c)^{1/2}$ and L_{xz}/d_c as well as the advection length scale L_{xx}/d_c (Fig. 5E). The turbulence intensities were consistently larger for the larger step heights (Fig. 5A) with differences of about 20–40%. The observations of integral turbulent time and length scales were identical with the findings of Felder and Chanson [25]. The observation was consistent with the lesser number of entrained air bubbles for the smallest step height since a dimensionless linear relationship between bubble count rate and turbulence intensities existed [26].

The comparative analysis of dimensionless auto- and cross-correlation integral time scales showed slightly larger time scales for the smallest step height (Fig. 5D). The differences were seen for the entire air-water flow column. Stronger scatter was observed for the transition flow data (Fig. 5D). The differences in auto- and cross-correlation time scale distributions were consistent with observations of the auto- and cross-correlation functions. It appeared that a scaling of the time scales to prototype scale was not possible using a Froude similitude. A similar result was observed in terms of the dimensionless integral turbulent time and lengths scales and for the dimensionless advection turbulent length scale (Fig. 5E). Overall, the results implied scale effects for a Froude similitude in terms of the large turbulence flow structures and in terms of the air-water flow interactions on the microscopic scale highlighting the importance to base the scaling of air-water flows not just on rough parameters of void fraction and interfacial velocity.

Fig. 6 illustrates the comparison of particle chord size probability distribution functions for the two scaled stepped spillways. The comparative analysis showed strong differences in terms of the dimensionless chord sizes of both air bubbles (Fig. 6A) and water droplets (Fig. 6B). For all data, the dimensionless chord sizes showed a greater number of smaller chord sizes for the largest step heights and a greater number of larger chord sizes for the smallest step heights. The Froude similitude did not scale the bubble and droplet chord sizes, confirming previous observations by Chanson and Gonzalez [17] and Felder and Chanson [25]. It was consistent with statements of Kobus [34] who expressed that scaling of entrained air bubble sizes is nearly impossible. Experiments based on a Weber similitude might scale the bubble sizes better, but the gravity and viscous forces are more important in physical modelling of stepped spillways.

As identified in Section 3, the near-wake criterion provided most suitable results in terms of microscopic cluster properties. For the range of cluster properties, detailed comparison of experimental results were performed for the two scaled spillway models. Fig. 7 illustrates the comparative analysis as a function of void frac-

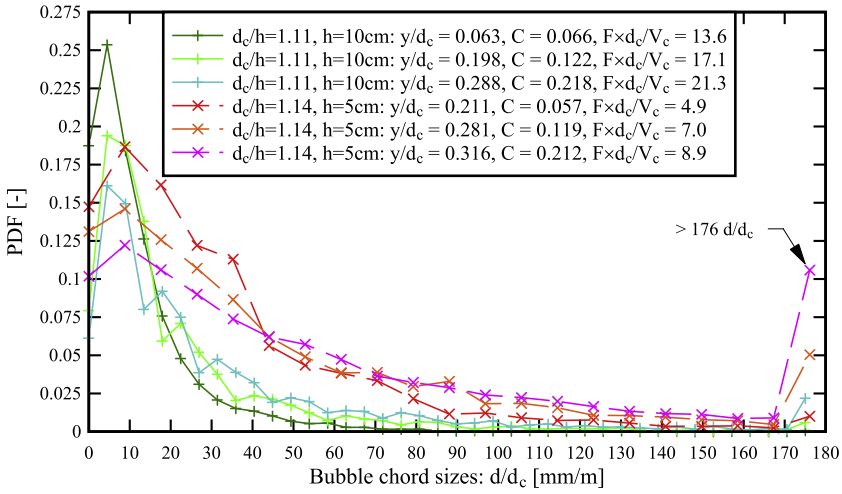

(A) Probability distribution function of air bubble chord sizes

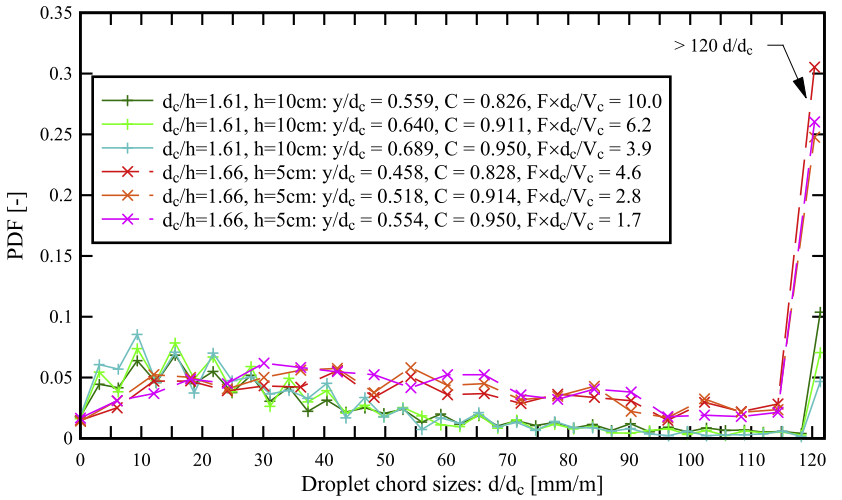

(B) Probability distribution function of water droplet chord sizes

Fig. 6. Comparison of microscopic air-water flow properties based upon Froude similitude: chord sizes.

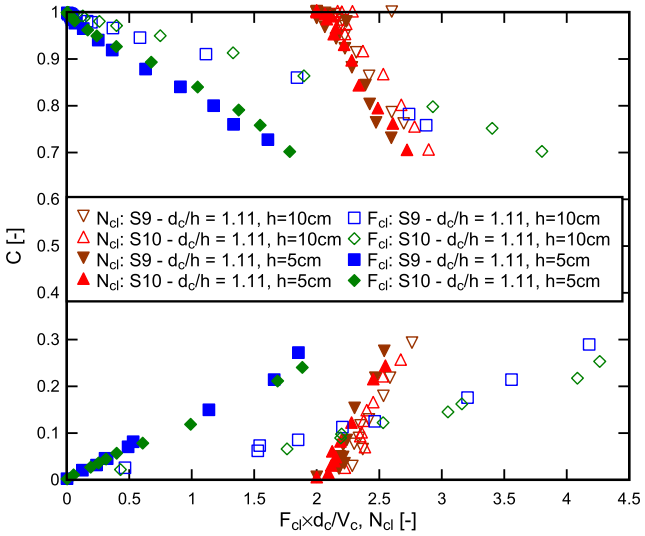

(A) Number of clusters per second F_{cl} and average number of particles per cluster N_{cl}

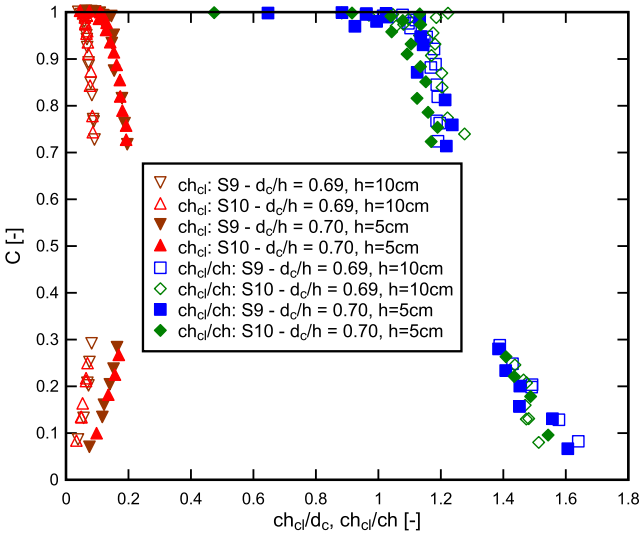

(B) Average chord sizes of particles in cluster ch_{cl} and ratio average chord size of cluster particles ch_{cl} to average chord size ch

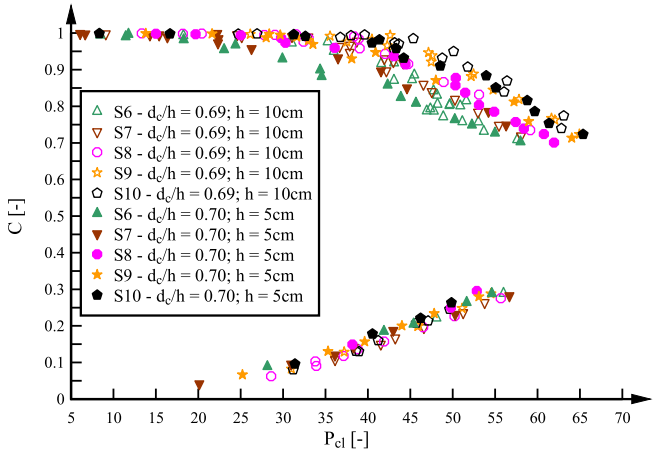

(C) Percentage of particles in clusters P_{cl}

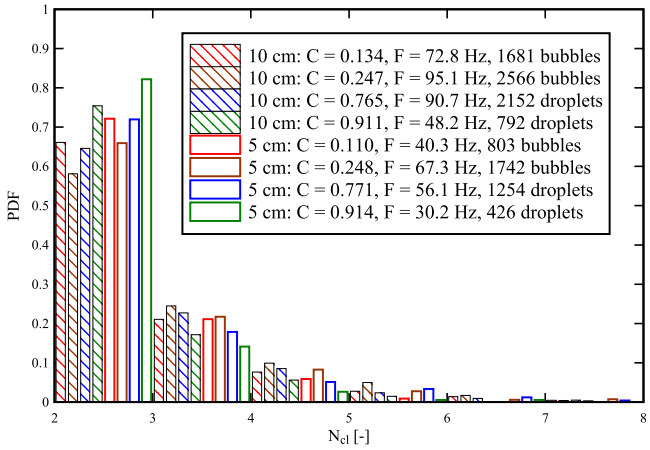

(D) PDF of average number of particles per cluster N_{cl} (d_c/h = 1.61, h =0.1 m; d_c/h = 1.66, h =0.05 m)

Fig. 7. Comparison of microscopic air-water flow properties based upon Froude similitude: cluster properties.

tion highlighting significant scale effects in terms of several dimensionless cluster properties for both transition and skimming flows. In Fig. 7A, strong scale effects are shown in terms of the dimensionless number of clusters per second $F_{cl} \times d_c/V_c$ with about double the number of clusters for the larger step height throughout the cross-section. The number of clusters per second could not be scaled accurately with a Froude similitude. Smaller scale effects were observed in terms of the number of bubbles/droplets per cluster which showed a larger number for the largest step heights (Fig. 7A).

Differences between the two configurations were also seen in terms of the dimensionless bubble/droplet chord sizes of particles in clusters ch_{cl}/d_c (Fig. 7B). The dimensionless chord sizes for the smallest step height were larger compared to the largest step height. This finding was consistent with the larger dimensionless chord sizes reported in the PDF distributions of air bubble and water droplet chord sizes (Fig. 6). The ratio of average cluster chord sizes of particles in clusters and average chord sizes showed little differences between the two scaled configurations (Fig. 7B). The comparative analyses showed further a slightly larger percentage of bubbles/droplets in clusters P_{cl} for the largest step height (Fig. 7C). In Fig. 7D, the probability distribution functions of average number of particles per cluster are shown for the two step heights indicating a slightly larger number of smaller particles for the smallest step heights. Overall, the comparative analysis of the cluster properties based upon a Froude similitude showed scale effects for several parameters. The findings confirmed that air-water flow properties on a microscopic scale were not properly scaled by a Froude similitude. An extrapolation of the results to a prototype scale is not possible.

Potential scale effects in terms of the interparticle arrival time t_{ipa} were also investigated. The interparticle arrival time provided information about the randomness of the travelling particles [23,32,10]. Herein, the particles were split into classes of particle chord sizes for which a similar behaviour may be expected [23]. For each class, the PDF of the dimensionless interparticle arrival time $t_{ipa} \times (g/d_c)^{1/2}$ between successive bubbles/droplets was calculated and compared between the two step height configurations

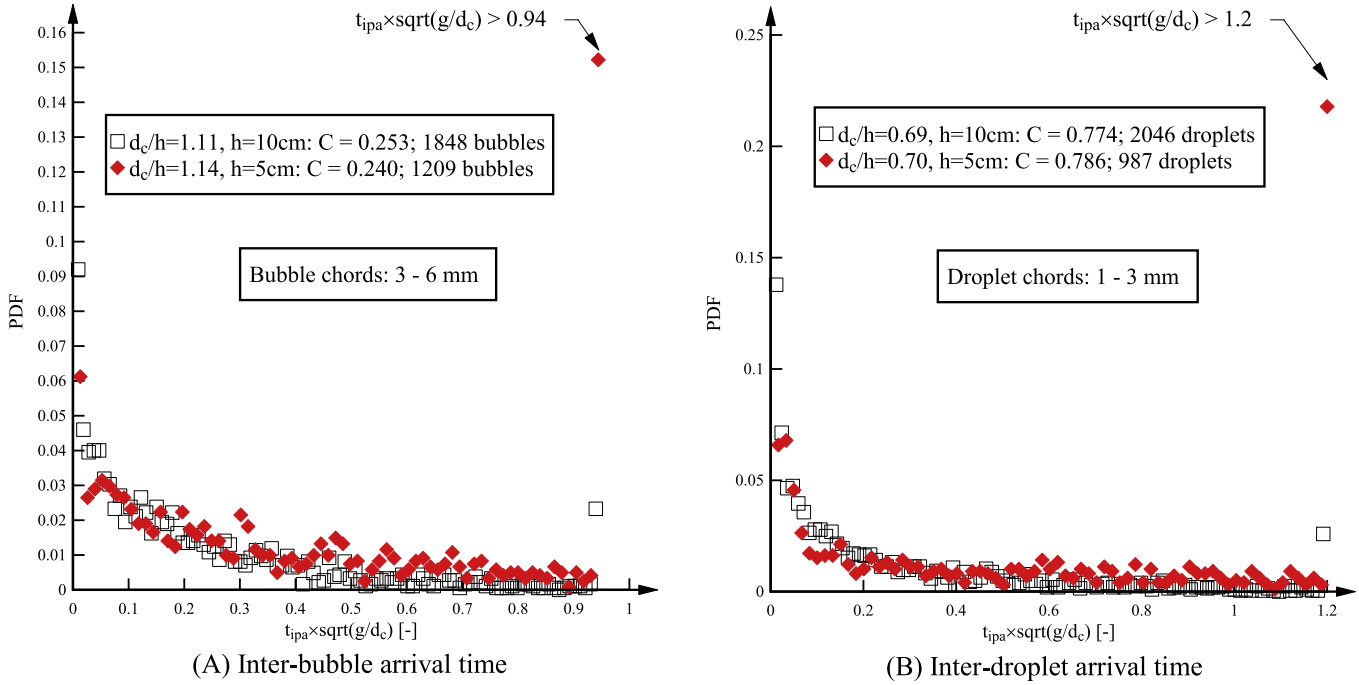

Fig. 8. Comparison of microscopic air-water flow properties based upon Froude similitude: interparticle arrival times.

(Fig. 8). Fig. 8 illustrates some typical distributions for bubble and droplet chord classes. For all experiments, smaller dimensionless inter-particle arrival times were more likely for the larger step heights, while larger dimensionless inter-particle arrival times appeared more often for the configuration with smaller step heights. Interestingly the differences between the two step heights decreased with increasing chord size classes for both air bubbles and water droplets and for all flow configurations. The comparative analysis indicated that the inter-particle arrival times between air bubbles and water droplets cannot be scaled properly with a Froude similitude.

4.2. Reynolds similitude

The full range of air-water flow properties was also investigated for the two step heights based upon a Reynolds similitude, i.e. the Reynolds numbers were identical in both stepped configurations. The comparative analyses comprised a range of flow conditions in both transition and skimming flows (Table 3) at step edges with same distance downstream from the inception point. Scale effects were observed for several air-water flow properties and typical results are illustrated in Fig. 9 as a function of y/d_c.

In Fig. 9A, the void fraction distribution is illustrated showing a relatively close agreement between the two scaled models. This finding was consistent with the observations by Felder and Chanson [25] confirming the scalability of void fraction based upon a Reynolds similitude. All other properties however showed scale effects highlighting that the majority of characteristic air-water flow parameters could not be extrapolated to a prototype scale based upon the Reynolds scaling criterion. Several properties showed some significant scale effects including the turbulence intensity (Fig. 9A), as well as the bubble count rate and interfacial area (Fig. 9C). For all data sets, the turbulence levels for the larger step height exceeded the levels for the smaller step heights by 30–60% (Fig. 9A), the dimensionless bubble count rates were about twice for the larger step heights (Fig. 9C) and the dimensionless interfacial area were about 10–30% larger. The present results highlighted that several important properties characterising the air-water interface and the fast fluctuating particle motions were not properly scaled indicating that air-water mass transfer processes as well as energy dissipation mechanisms may not be accurately scaled.

Fig. 9B shows typical dimensionless distributions of maximum cross-correlation coefficients and interfacial velocities. For both air-water flow properties, some differences were observed independent of the flow conditions with slightly larger cross-correlation coefficients for the smaller step heights and larger interfacial velocities for the larger step heights. Small scale effects were also observed in terms of the auto- and cross-correlation time scales (Fig. 9D) as well as the transverse integral turbulent time and length scales and the advection length scale (Fig. 9E). For all characteristic dimensionless time and length scales, the data for the largest step heights were slightly larger. The finding of only small differences in transverse integral turbulent time and length scales differed from the observations of Felder and Chanson [25] who showed larger differences in scales. Overall the scaling of several key air-water flow properties to the prototype size was not possible using the Reynolds similitude.

Significant scale effects were also observed in terms of several characteristic microscopic air-water flow properties highlighting that the small scale interactions between air and water entities cannot be accurately scaled with a Reynolds similitude. In Fig. 10, typical dimensionless air bubble and water droplet chord size distributions are compared for the two stepped spillway configurations. The PDF distribution of bubble chord sizes showed comparatively smaller chord sizes for the largest step heights (Fig. 10A). A similar finding was also observed for the water droplet chord sizes, with smallest chords for the largest step heights (Fig. 10B). The scaling of the chord sizes to prototype scale was not possible using the Reynolds similitude even though the scaling was overall better compared to the Froude similitude.

Similarly scale effects were observed in terms of several cluster properties including the dimensionless number of cluster per second with a cluster count rate twice as large for the largest step height (Fig. 11A). The differences in average number of particles per cluster reflected on average larger numbers of particles for

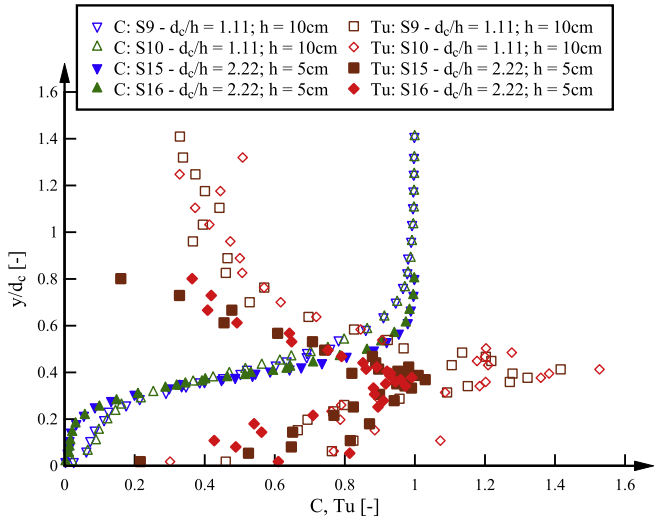

(A) Void fraction and turbulence intensity

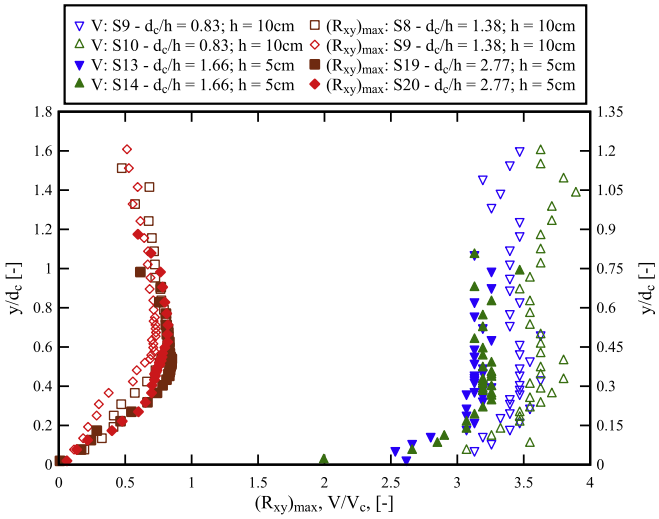

(B) Maximum cross-correlation coefficient and interfacial velocity

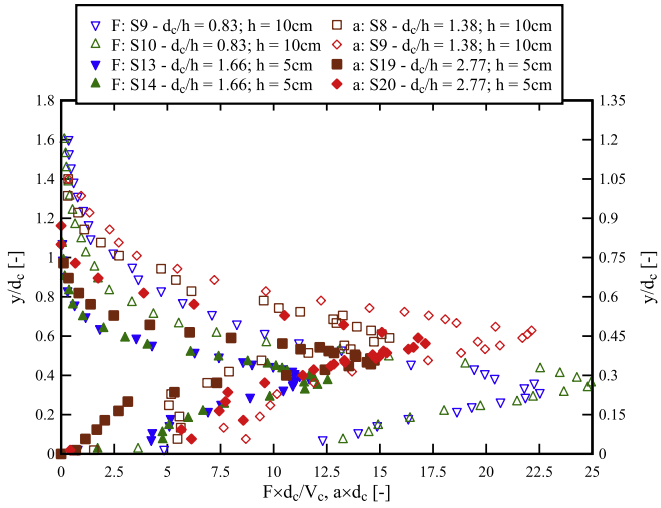

(C) Bubble count rate and interfacial area

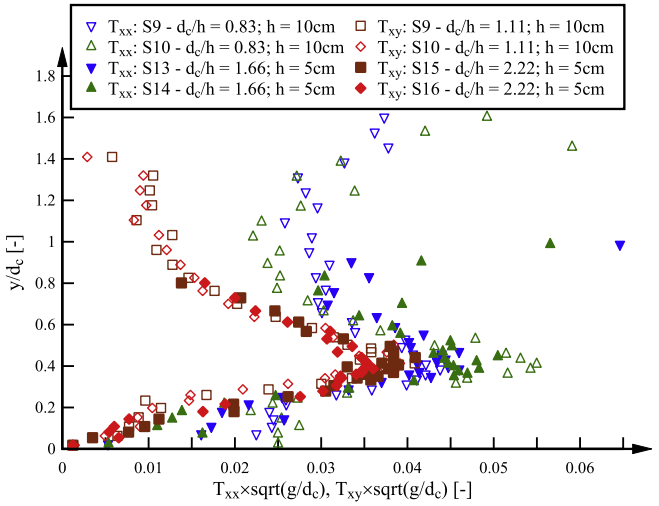

(D) Auto- and cross-correlation time scales

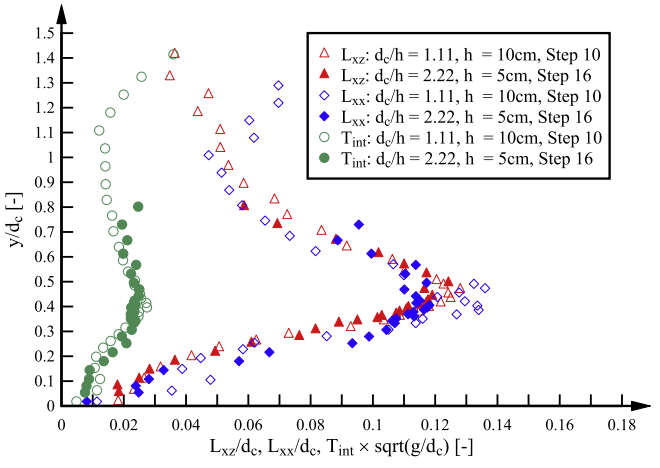

(E) Transverse integral turbulent time and length scales; advection length scale

Fig. 9. Comparison of air-water flow properties based upon Reynolds similitude.

the largest step height. While the dimensionless average chord sizes of particles in clusters were almost identical for the two step heights, the ratio of average chord size of cluster particles to average chord sizes was about 10–20% larger for the largest step heights (Fig. 11B). Similarly a slightly larger percentage of particles in clusters was observed for the stepped spillway with h = 0.1 m

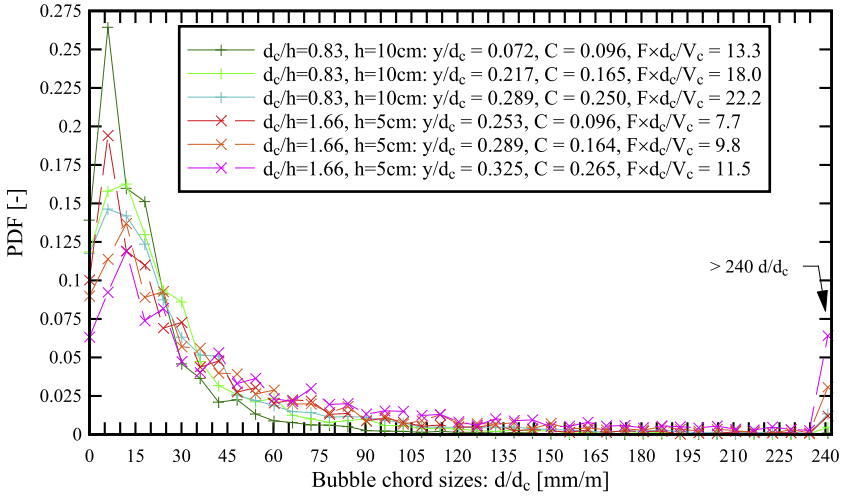

(A) Probability distribution function of air bubble chord sizes

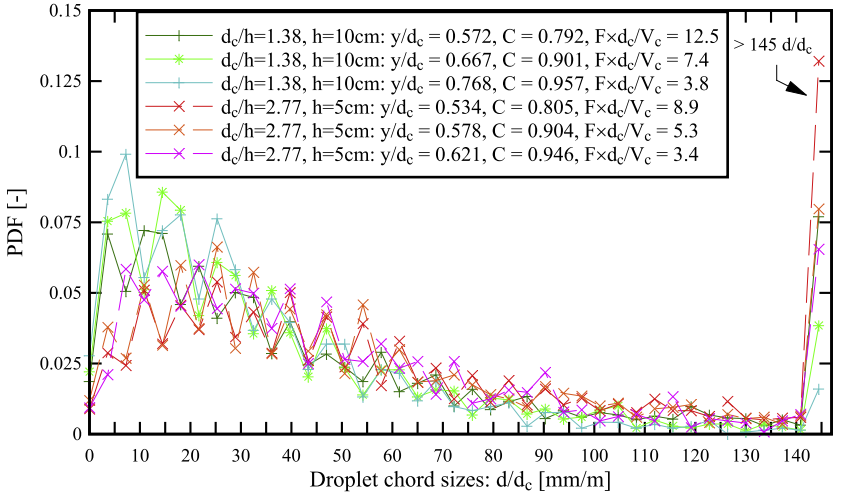

(B) Probability distribution function of water droplet chord sizes

Fig. 10. Comparison of microscopic air-water flow properties based upon Reynolds similitude: chord sizes.

(Fig. 11C). The comparison of PDF of average number of particles per cluster showed a slightly larger proportion of smaller particles per cluster for the smaller step height (Fig. 11D). The observation of these cluster properties indicated scale effects for the Reynolds similitude.

The comparative analysis of dimensionless interparticle arrival times is shown in Fig. 12 for typical air bubble chord sizes (Fig. 12A) and water droplet chord sizes (Fig. 12B). The data showed consistently a proportionally larger number of smaller interparticle arrival times for the largest step height and a larger number of larger interparticle arrival times for the smallest step heights independent of bubble or droplet chord classes (Fig. 12). With increasing chord size classes, the differences decreased for both air bubble and water droplet chords. Overall, the present results confirmed significant scale effects for a Reynolds similitude which highlighted the difficulty to scale the air-water flow properties accurately.

4.3. Discussion

The application of the classical dynamic similarity approach was not successful to scale most air-water flow properties on stepped spillway models with geometrically scaled step heights. Neither the Froude nor the Reynolds similitudes could be used to scale the air-water flow properties accurately to a prototype scale. A detailed comparative analysis was conducted for experimental results on two geometrically scaled stepped spillway models with $\theta = 26.6°$. The full range of air-water flow properties was tested for both Froude and Reynolds similitudes and significant scale effects were found. Table 4 summarises the outcomes of the present study including the wide range of macro- and microscopic air-water flow properties tested and the large number of parameters affected by scale effects. The results highlighted that a proper scaling of the air-water flows on geometrically scaled stepped spillways is not possible using either the Froude or Reynolds similitudes. While similar findings were previously reported by Chanson and Gonzalez [17] and Felder and Chanson [25], the present study encompassed a much broader range of air-water flow properties for a wide range of flow conditions in transition and skimming flow regimes. Table 4 provides a detailed summary of all air-water flow properties affected by scale effects highlighting that only the void fraction and the interfacial velocity may be properly scaled for the investigated flow range ($Re > 8 \times 10^4$). It is believed that the present investigation on a stepped spillway provides some clear guidance for possible scale effects in further air-water flows with violent air entrainment process through the free-surface including

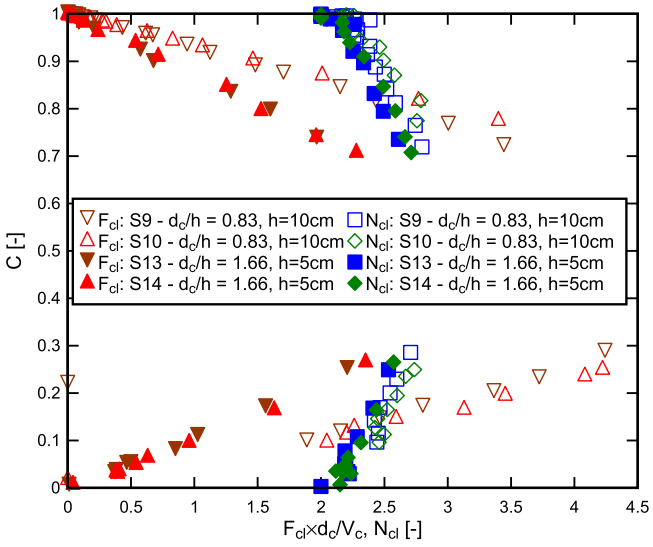

(A) Number of clusters per second F_{cl} and average number of particles per cluster N_{cl}

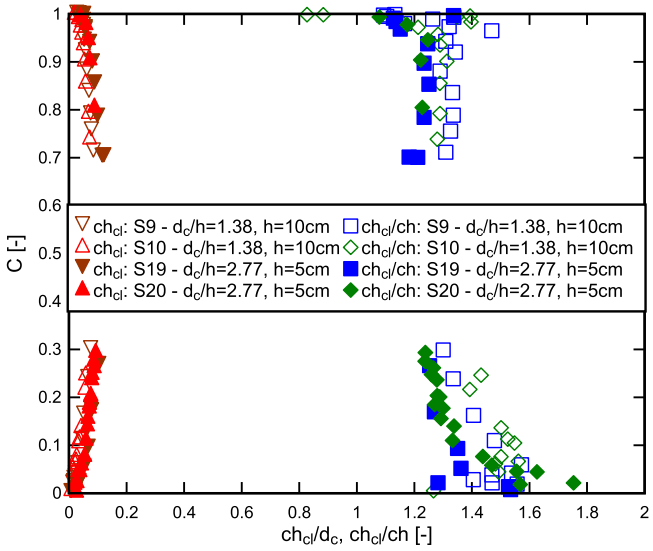

(B) Average chord sizes of particles in cluster ch_{cl} and ratio average chord size of cluster particles ch_{cl} to average chord size ch

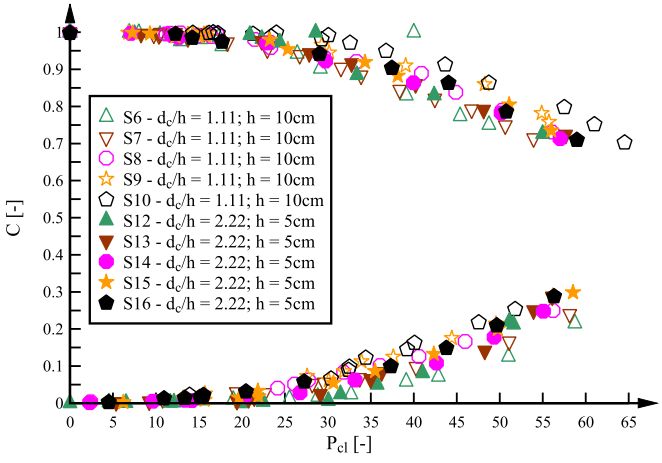

(C) Percentage of particles in clusters P_{cl}

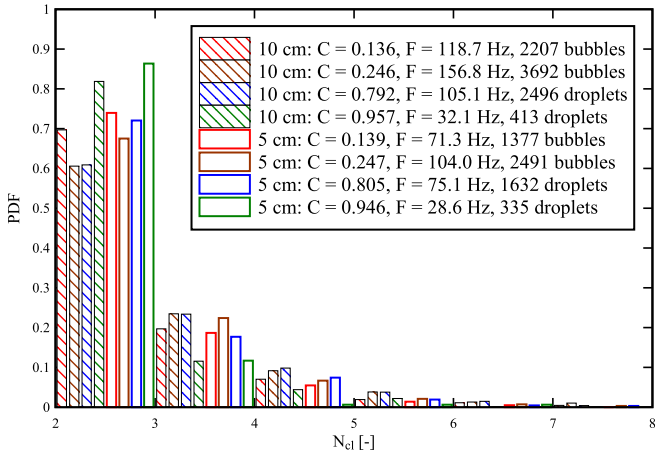

(D) PDF of average number of particles per cluster N_{cl} (d_c/h = 1.38, h =0.1 m; d_c/h = 2.77, h =0.05 m)

Fig. 11. Comparison of microscopic air-water flow properties based upon Reynolds similitude: cluster properties.

hydraulic jumps, ski jumps, drop structures as well as breaking waves. The findings of several systematic experimental studies including the present one demonstrated that the notion of scale effects must be defined in terms of very specific set of air-water flow property(ies), and some aerated flow properties are more affected by scale effects than others, even in large-size facilities.

The present study was conducted in the same experimental facility and with the same instrumentation. The key parameters which were varied were the step heights and the flow rates, but the channel width, the spillway material and its micro-roughness remained unchanged. While stepped spillway flows are dominated by drag resistance, scaling of the micro-roughness may impact upon the flow processes close to the invert of a hydraulic structure [29]. Further the instrumentation for both step configurations was identical including identical diameters of the conductivity probe sensors. The sensor size limits the measurable sizes of the smallest air and water entities affecting in particular the microscopic air-water flow properties. A future study should investigate the effect of sensor size to clarify any limitations and it is recommended to conduct a study with equivalent scaling ratio for both step and conductivity sensor sizes. The present study was conducted with a constant single threshold technique of 50% following the findings of Felder and Chanson [27]. Different other threshold techniques exist as summarised by Cartellier and Achard [8] which could result in minor variations in air-water flow properties. While the testing of scale effects could be conducted with a different threshold technique or single-threshold value, the finding of the present study would be similar if the threshold technique is equally applied to both step configurations. The comparative analyses of scale effects in the present study were based upon a scaling ratio of 1:2 and a comparison of air-water flow properties in Froude and Reynolds similitude should be also expanded to a larger range of scaling ratios.

While a range of air-water flows properties were not scalable to prototype scale (Table 4), self-similar relationships were found for all air-water flow properties which allowed a characterisation of

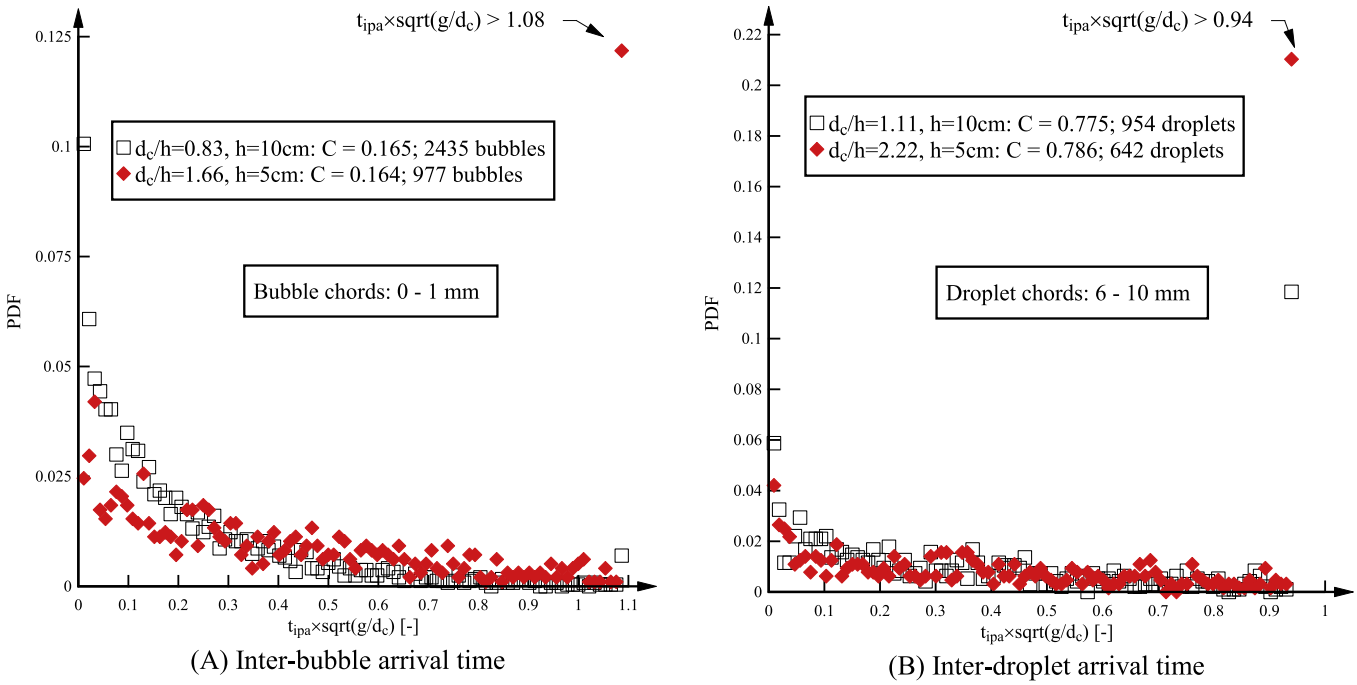

Fig. 12. Comparison of microscopic air-water flow properties based upon Reynolds similitude: interparticle arrival times.

Table 4
Summary of scale effects for Froude and Reynolds similitudes in high-velocity free-surface flows on a geometrically scaled stepped spillway (θ = 26.6°).

Air-water flow property	Scale effects in Froude similutude	Scale effects in Reynolds similutude
Void fraction	*No scale effects*	*No scale effects*
Bubble count rate	**Scale effects**	**Scale effects**
Interfacial velocity	*No scale effects*	Small scale effects
Turbulence intensity	**Scale effects**	**Scale effects**
Interfacial aeration	**Scale effects**	**Scale effects**
Auto-correlation function	Small scale effects	Small scale effects
Cross-correlation function	Small scale effects	Small scale effects
Maximum cross-correlation coefficient	*No scale effects*	Small scale effects
Auto-correlation time scale	Small scale effects	Small scale effects
Cross-correlation time scale	Small scale effects	Small scale effects
Integral turbulent length scales	**Scale effects**	Small scale effects
Integral turbulent time scales	**Scale effects**	Small scale effects
Advection turbulent length scale	Small scale effects	Small scale effects
Air bubble chord sizes	**Scale effects**	**Scale effects**
Water droplet chord sizes	**Scale effects**	**Scale effects**
Cluster properties	**Scale effects**	**Scale effects**
Inter-particle arrival time	**Scale effects**	**Scale effects**

the air-water flows independent of the physical scale. The self-similarity approach is a powerful tool in complex turbulent flows since it is based upon mathematical scaling [4]. It was previously successfully used by Chanson and Carosi [15] and Felder and Chanson [25] and recently expanded by Felder [24] to encompass the full range of air-water flow properties independent of step height and channel slope. While the detailed equations are not provided in this manuscript, the concept of self-similarity seems a powerful tool. However, prototype scale experiments are needed to confirm the self-similar relationships and to validate the laboratory studies of the past and present.

5. Conclusion

An experimental study of air-water flow properties was conducted on two stepped spillway configurations with scaling ratio of 2:1, i.e. step heights of h = 0.10 m & 0.05 m. The experiments were conducted for a range of discharges in transition and skimming flows using phase detection intrusive probes. The post-processing provided a wide range of air-water flow properties at both macroscopic and microscopic scale. For the cluster properties, several cluster criteria were tested to identify the most appropriate cluster criterion for air-water flows. The near-wake criterion was found most suitable because it linked the clusters to the local air-water flow features and provided a close relationship between numbers of particles in the flow and number of clusters per second.

For the full range of air-water flow properties, scale effects were systematically investigated based upon undistorted Froude and Reynolds similitudes. The comparative analyses confirmed that a scaling of void fraction and time-averaged interfacial velocities is possible for both types of similitude in a scaled model of 1:2. This finding is significant because it indicates that several important design parameters may be scaled correctly including the equivalent clear water flow depth, the flow bulking, the energy dissipation along the stepped chute and the residual energy at the downstream end of the spillway in a scale ratio of 1:2. However several further parameters were not properly scaled including the bubble count rate, interface area, turbulence intensities and correlation time scales. Furthermore the microscopic air-water flow properties comprising particle chord sizes, cluster properties and inter-particle arrival time could not be accurately scaled. These observations highlighted that the turbulence motion, the bubble sizes and the interfacial area, are very prone to scale effect, affecting the extrapolation of the air-water mass transfer processes.

The present finding emphasised explicitly that any notion of scale effects must be defined explicitly in terms of specific set of air-water flow property(ies) as illustrated in Table 4. Some air-water flow parameters are more affected by scale effects than others, even in large-size facilities. The present study provided clear guidelines of air-water flow properties which may experience

scale effects. Considering the broad range of flow conditions in the present study, these guidelines may be also applicable to further air-water flows. In general a detailed study of air-water flow properties at the prototype scale is needed to further confirm scaling guidelines in air-water flows.

Appendix A

Experimental studies of scale effects in stepped spillway flows

Reference	θ (deg.)	W (m)	h (m)	d_c/h	Re	Instrumentation	Measurements
BaCaRa [3]	53.1	–	0.012	–	–	Visual observations	
		0.56	0.024	0.7–3.8	0.27×10^5 to 3.7×10^5	Visual observations	
		0.90	0.028	–	–	Visual observations	
		0.75	0.060	0.7–1.75	0.98×10^5 to 3.8×10^5	Micro-propeller, Piezo-resistivity pressure sensors	Velocity, invert pressure
Boes [5]	30.0	0.50	0.023	1.4–5.2	4.8×10^5 to 1.1×10^6	Double-tip optical fibre probe	Void fraction, velocity
			0.046				
			0.092				
	50.0	0.50	0.031	0.8–2.4	2.4×10^5 to 1.1×10^6		
			0.093				
Chanson and Toombes [20]	3.4	0.50	0.0715	0.92–1.2	2.4×10^5 to 8.8×10^5	Single-tip conductivity probe (Ø = 0.35 mm)	Void fraction, bubble count rate
			0.143				
Chanson and Gonzalez [17]	15.9	1.0	0.050	0.87–1.7	1.2×10^5 to 1.2×10^6	Double-tip conductivity probe (Ø = 0.025 mm)	Void fraction, bubble count rate, velocity, turbulence intensity, bubble sizes
			0.100				
Relvas and Pinheiro [39]	21.8	0.270	0.030	0.9–3.7	0.83×10^5 to 1.4×10^6	Double-tip optical probe	Void fraction
		0.67	0.074				
Bung [7]	18.4	0.30	0.030	1.3–3.6	2.8×10^5 to 4.4×10^5	Double-tip conductivity probe (Ø = 0.13 mm)	Void fraction, bubble count rate, velocity
	26.6		0.060				
Felder and Chanson [25]	21.8	1.0	0.050	0.18–3.5	0.32×10^5 to 8.3×10^5	Double-tip conductivity probe (Ø = 0.25 mm), array of single-tip conductivity probe (Ø = 0.35 mm)	Void fraction, bubble count rate, velocity, turbulence intensity, bubble sizes, integral turbulent time and length scales
			0.100				
Present study	26.6	1.0	0.050	0.7–3.3	0.81×10^5 to 9.0×10^5	Double-tip conductivity probe (Ø = 0.25 mm), array of single-tip conductivity probe (Ø = 0.35 mm)	Void fraction, bubble count rate, velocity, turbulence intensity, bubble sizes, integral turbulent time and length scales, correlation time scales, interfacial area, clustering, interparticle arrival time
			0.100				

Notes: θ: chute slope; W: chute width; h: vertical step height; d_c: critical flow depth; Re: Reynolds number defined in terms of the hydraulic diameter; (–): information not available.

References

[1] A. Amador, M. Sanchez-Juny, J. Dolz, DPIV Study of the turbulent boundary layer over V-shaped cavities, in: R.M.L. Ferreira, E.C.T.L. Alves, J.G.A.B. Leal, A.H. Cardoso, (Eds.), Proceeding International Conference on Fluvial Hydraulics River Flow 2006, Lisbon, Portugal, 6–8 September, Topic A1, vol. 2, Balkema Publishing, Taylor & Francis Group, London, 2006, pp. 1813–1821.

[2] S. Andre, J.L. Boillat, A. Schleiss, Two-phase flow characteristics of stepped spillways discussion, J. Hydraulic Eng., ASCE 131 (5) (2005) 423–427.

[3] BaCaRa, Etude de la Dissipation d'Energie sur les Evacuateurs à Marches. (Study of the Energy Dissipation on Stepped Spillways.) Rapport d'Essais, Projet National BaCaRa, CEMAGREF-SCP, Aix-en-Provence, France, October, 1991, p. 111 (in French).

[4] G.I. Barenblatt, Scaling, Self-Similarity, and Intermediate Asymptotics, Cambridge University Press, 1996, p. 386.

[5] R.M. Boes, Scale effects in modelling two-phase stepped spillway flow, in: Proc. of the International Workshop on Hydraulics of Stepped Spillways, Balkema, 2000, pp. 53–60.

[6] F.A. Bombardelli, I. Meireles, J. Matos, Laboratory measurements and multiblock numerical simulations of the mean flow and turbulence in the non-aerated skimming flow region of steep stepped spillways, Environ. Fluid Mech. 11 (2011) 263–288.

[7] D.B. Bung, Zur selbstbelüfteten Gerinnenströmung auf Kaskaden mit gemässigter Neigung, in: Self-Aerated Skimming Flows on Embankment Stepped Spillways, University of Wuppertal, LuFG Wasserwirtschaft and Wasserbau, Germany, 2009, p. 292, Ph.D. thesis, (in German).

[8] A. Cartellier, J.L. Achard, Local phase detection probes in fluid/fluid two-phase flows, Rev. Sci. Instrum. 62 (1991) 279–303.

[9] H. Chanson, The Hydraulics of Stepped Chutes and Spillways, Balkema, Lisse, The Netherlands, 2001 (ISBN 90 5809 352 2).

[10] H. Chanson, Advective diffusion of air bubbles in turbulent water flows, in: C. Gualtieri, D.T. Mihailovic (Eds.), Fluid Mechanics of Environmental Interfaces, Taylor & Francis, Leiden, The Netherlands, Chapter 7, 2008, pp. 163–196.

[11] H. Chanson, Turbulent air-water flows in hydraulic structures: dynamic similarity and scale effects, Environ. Fluid Mech. 9 (2) (2009) 125–142.

[12] H. Chanson, Convective transport of air bubbles in strong hydraulic jumps, Int. J. Multiph. Flow 36 (10) (2010) 798–814, http://dx.doi.org/10.1016/j.ijmultiphaseflow.2010.05.006) (ISSN 0301-9322).

[13] H. Chanson, Hydraulics of aerated flows: qui pro quo?, J Hydraulic Res., IAHR, Invited Vision Paper 51 (3) (2013) 223–243, http://dx.doi.org/10.1080/00221686.2013.795917.

[14] H. Chanson, S. Aoki, A. Hoque, Bubble entrainment and dispersion in plunging jet flows: freshwater versus seawater, J. Coastal Res. 22 (3) (2006) 664–677.

[15] H. Chanson, G. Carosi, Turbulent time and length scale measurements in high-velocity open channel flows, Exp. Fluids 42 (3) (2007) 385–401.

[16] H. Chanson, Y. Chachereau, Scale effects affecting two-phase flow properties in hydraulic jump with small inflow Froude number, Exp. Therm. Fluid Sci. 45 (2013) 234–242.

[17] H. Chanson, C.A. Gonzalez, Physical modelling and scale effects of air-water flows on stepped spillways, J. Zhejiang Univ. Sci. 6A (3) (2005) 243–250.

[18] H. Chanson, L. Toombes, Strong interactions between free-surface aeration and turbulence down a staircase channel, in: Proc. 14th Australasian Fluid Mech. Conf., Adelaide, Australia, 2001, pp. 841–844.

[19] H. Chanson, L. Toombes, Air-water flows down stepped chutes: turbulence and flow structure observations, Int. J. Multiph. Flow 28 (11) (2002) 1737–1761.

[20] H. Chanson, L. Toombes, Energy dissipation and air entrainment in a stepped storm waterway: an experimental study, J. Irrigation Drainage Eng., ASCE 128 (5) (2002) 305–315.

[21] X.J. Cheng, Y.C. Chen, L. Luo, Numerical simulation of air-water two-phase flow over stepped spillways, Sci. China Ser. E – Technol. Sci. 49 (6) (2006) 674–684.

[22] R. Clift, J.R. Grace, M.E. Weber, Bubbles, Drops, and Particles, Academic Press, San Diego, 1978, 380.

[23] C.F. Edward, K.D. Marx, Multipoint statistical structure of the ideal spray, Part II: Evaluating steadiness using the interparticle time distribution, At. Sprays 5 (1995) 435–455.

[24] S. Felder, Air-Water Flow Properties on Stepped Spillways for Embankment Dams: Aeration, Energy Dissipation and Turbulence on Uniform, Non-Uniform and Pooled Stepped Chutes. PhD Thesis, The University of Queensland, Australia, 2013, 506.

[25] S. Felder, H. Chanson, Turbulence, dynamic similarity and scale effects in high-velocity free-surface flows above a stepped chute, Exp. Fluids 47 (2009) 1–18.

[26] S. Felder, H. Chanson, Air-water flow properties in step cavity down a stepped chute, Int. J. Multiph. Flow 37 (7) (2011) 732–745.

[27] S. Felder, H. Chanson, Phase-detection probe measurements in high-velocity free-surface flows including a discussion of key sampling parameters, Exp. Therm. Fluid Sci. 61 (2015) 66–78.

[28] S. Felder, H. Chanson, Air–water flow characteristics in high-velocity free-surface flows with 50% void fraction, Int. J. Multiph. Flow 85 (2016) 186–195.

[29] S. Felder, N. Islam, Hydraulic performance of an embankment weir with rough crest, J. Hydraulic Eng. 12 (2016) 04016086, http://dx.doi.org/10.1061/(ASCE)HY.1943-7900.000125.

[30] C. Gualtieri, H. Chanson, Clustering process and interfacial area analysis in a large-size dropshaft, Proc. 5th International Conference Advances in Fluid Mechanics (AFM 2004), vol. V, Advances in Fluid Mechanics, Lisbon, Portugal, 2004, pp. 415–424.

[31] C. Gualtieri, H. Chanson, Effect of Froude number on bubble clustering in a hydraulic jump, J. Hydraul. Res. 48 (4) (2010) 504–508.

[32] J. Heinlein, U. Fritsching, Droplet clustering in sprays, Exp. Fluids 40 (3) (2006) 464–472.

[33] V. Heller, Scale effects in physical hydraulic engineering models, J. Hydraul. Res. 49 (3) (2011) 293–306.

[34] H. Kobus, Local air entrainment and detrainment, in: Proc. Symp. on Scale Effects in Modelling Hydraulic Structures, IAHR, Esslingen, Germany, 1984.

[35] I. Meireles, F. Bombardelli, J. Matos, Experimental testing and numerical simulation of the non-aerated skimming flow over steeply sloping stepped spillways, Proc. 33rd IAHR Congress, Vancouver, Canada, 2009, pp. 1972–1979.

[36] I. Ohtsu, Y. Yasuda, Characteristics of flow conditions on stepped channels, in: Proc. 27th IAHR Biennial Congress, San Francisco, USA, Theme D, 1997, pp. 583–588.

[37] M. Pfister, H. Chanson, Two-phase air-water flows: scale effects in physical modeling, J. Hydrodynamics 26 (2) (2014) 291–298.

[38] N.S.L. Rao, H.E. Kobus, Characteristics of self-aerated free-surface flows, Water and Waste Water/Current Research and Practice, 10, Eric Schmidt Verlag, Berlin, Germany, 1971.

[39] A.T. Relvas, A.N. Pinheiro, Inception point and air concentration in flows on stepped chutes lined with wedge-shaped concrete blocks, J. Hydraulic Eng., ASCE 134 (8) (2008) 1042–1051.

[40] M.P. Schultz, K.A. Flack, Reynolds-number scaling of turbulent channel flow, Phys. Fluids 25 (2013), Paper 025104, p. 13.

[41] D. Valero, D.B. Bung, Hybrid investigations of air transport processes in moderately sloped stepped spillway flows, E-Proceedings of the 36th IAHR World Congress, The Hague, Netherlands, 2015.

[42] H. Wang, H. Chanson, Self-similarity and scale effects in physical modelling of hydraulic jump roller dynamics, air entrainment and turbulent scales, Environ. Fluid Mech. (2016), http://dx.doi.org/10.1007/s10652-016-9466-z.

[44] I.R. Wood, Air Entrainment in Free-Surface Flows, IAHR Hydraulic Structures Design Manual No. 4, Hydraulic Design Considerations, Balkema Publ., Rotterdam, The Netherlands, 1991, 149.